



# Formulation and development of composite materials for thermally driven and storage-integrated cooling technologies: a review

Emiliano Borri<sup>1</sup> · Svetlana Ushak<sup>2</sup> · Yongliang Li<sup>3</sup> · Andrea Frazzica<sup>4</sup> · Yannan Zhang<sup>4</sup> · Yanio E. Milian<sup>2</sup> · Mario Grageda<sup>2</sup> · Dacheng Li<sup>3</sup> · Luisa F. Cabeza<sup>1</sup> · Vincenza Brancato<sup>4</sup>

Received: 23 February 2024 / Accepted: 25 June 2024 / Published online: 15 July 2024  
© The Author(s) 2024

## Abstract

The energy consumption for cooling takes up 50% of all the consumed final energy in Europe, which still highly depends on the utilization of fossil fuels. Thus, it is required to propose and develop new technologies for cooling driven by renewable energy. Also, thermal energy storage is an emerging technology to relocate intermittent low-grade heat source, like solar thermal energy and industrial waste heat as well as to exploit off-peak electricity, for cooling applications. This review aims to summarize the recent advances in thermally driven cooling and cold storage technologies, focusing on the formation and fabrication of adopted composites materials, including sorption materials, phase change materials, and slurries. Herein, first the classifications, selection criteria, and properties for these three types of materials is discussed. Then, the application potentials of all the materials are prospected in terms of economic analysis and sustainability.

**Keywords** Phase change materials · Sorption sorbents · Slurries · Thermal energy storage · Cooling

## Introduction

To achieve EU climate neutrality by 2050 and worldwide climate change mitigation targets, decarbonization of the EU industries and the EU energy system are crucial.

EU industrial cooling accounts for 86 TWh/year, with 80% share coming from the demand in food and basic chemical industries at temperatures between – 30 °C and 15 °C

[1]. Today, such industries rely mostly on vapor compression systems to meet such cooling demand, nevertheless these industries are usually releasing a large amount of industrial waste heat (IWH), estimated to be around 160 TWh/year in EU and/or are located in sites with available renewable energy sources. Therefore, there is a big push to transform such status-quo by developing new cooling devices that

---

✉ Vincenza Brancato  
vincenza.brancato@cnr.it

Emiliano Borri  
emiliano.borri@udl.cat

Svetlana Ushak  
svetlana.ushak@uantof.cl

Yongliang Li  
y.li.1@bham.ac.uk

Andrea Frazzica  
d.li.6@bham.ac.uk

Yanio E. Milian  
yanio.milian@ua.cl

Mario Grageda  
mario.grageda@uantof.cl

Dacheng Li  
d.li.6@bham.ac.uk

Luisa F. Cabeza  
luisaf.cabeza@udl.cat

<sup>1</sup> GREiA Research Group, University of Lleida, 25001 Lleida, Spain

<sup>2</sup> Center for Advanced Study of Lithium and Industrial Minerals (CELiMIN), Departamento de Ingeniería Química y Procesos de Minerales, Universidad de Antofagasta, Campus Coloso, Av. Universidad de Antofagasta, 02800 Antofagasta, Chile

<sup>3</sup> Birmingham Centre for Energy Storage, School of Chemical Engineering, University of Birmingham, Edgbaston, Birmingham B15 2TT, UK

<sup>4</sup> CNR ITAE, Istituto Di Tecnologie Avanzate Per L'Energia "Nicola Giordano", Via Santa Lucia Sopra Contesse, 5, 98126 Messina, Italy

include renewable/thermally driven and storage-integrated cooling technologies.

Cooling technologies that include renewable/thermally driven and storage-integrated cooling technologies are based on either sorption technologies or storage technologies, mostly thermal energy storage based on phase change materials (PCMs). But literature shows that using sorption materials or PCMs as such show low efficiency and more important, low thermal cycling stability [2, 3], therefore this paper focuses on composites and slurries. During the last 5 years, the published research activities related to the development of material for low temperature thermal

energy storage are not that frequent as medium and high temperature investigations.

Figure 1 shows the co-occurrence of keywords elaborated with the software VOSviewer of the documents published until 2023 related to sorbents for TES applications. Two different query were used to retrieve data from the Scopus database to search studies related to sorbents for general TES applications TITLE-ABS-KEY (“thermal energy storage” OR “thermal storage”) AND (sorbent\*). Results highlights that the main applications of sorbents as TES are mainly for solar energy.

The co-occurrence of the keywords of studies related to composite PCM for TES is shown in Fig. 2. The query

**Fig. 1** Co-occurrence of key-words elaborated with the software VOSviewer for sorbents for TES applications

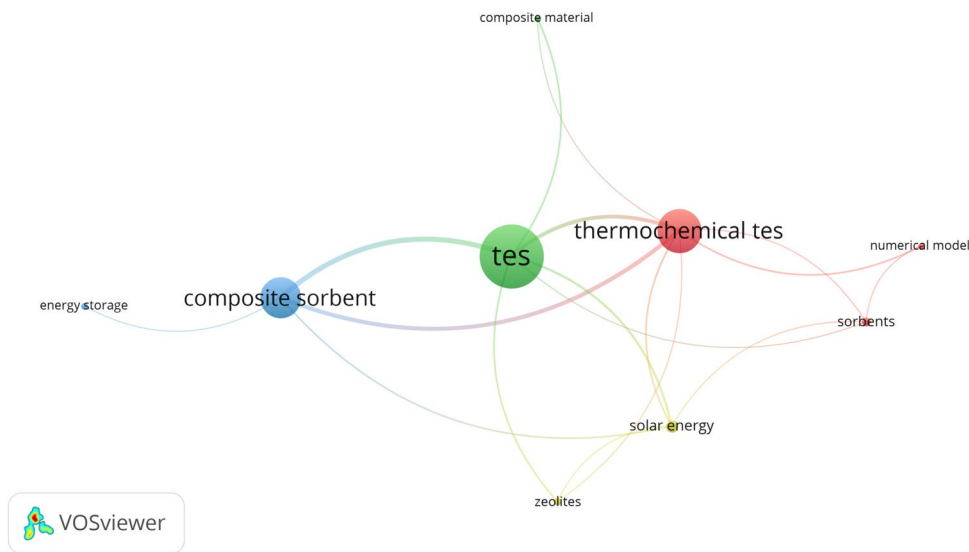


**Fig. 2** Co-occurrence of key-words elaborated with the software VOSviewer for composite PCMs for TES applications

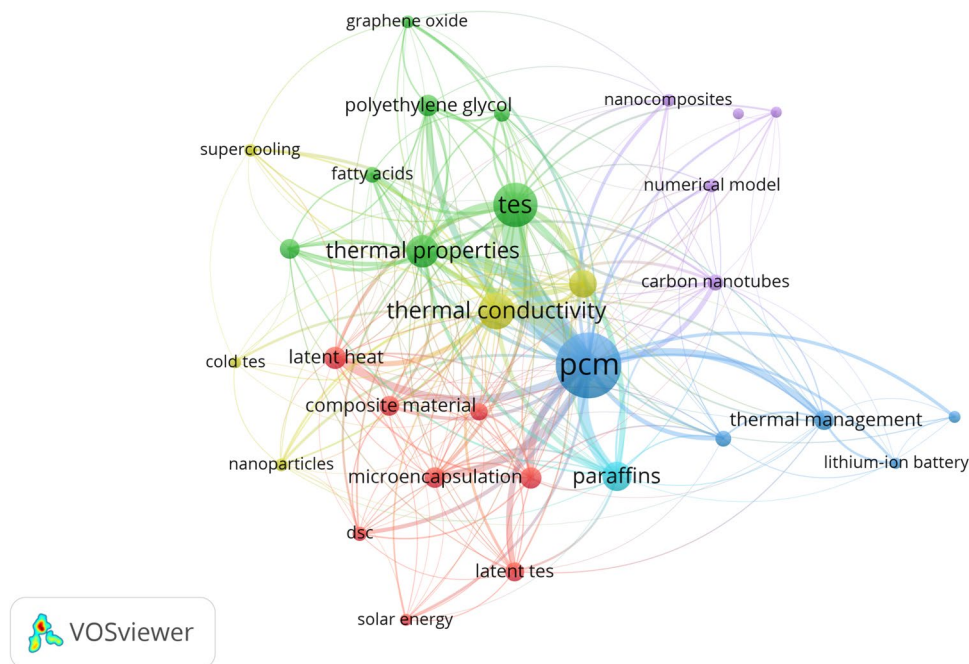
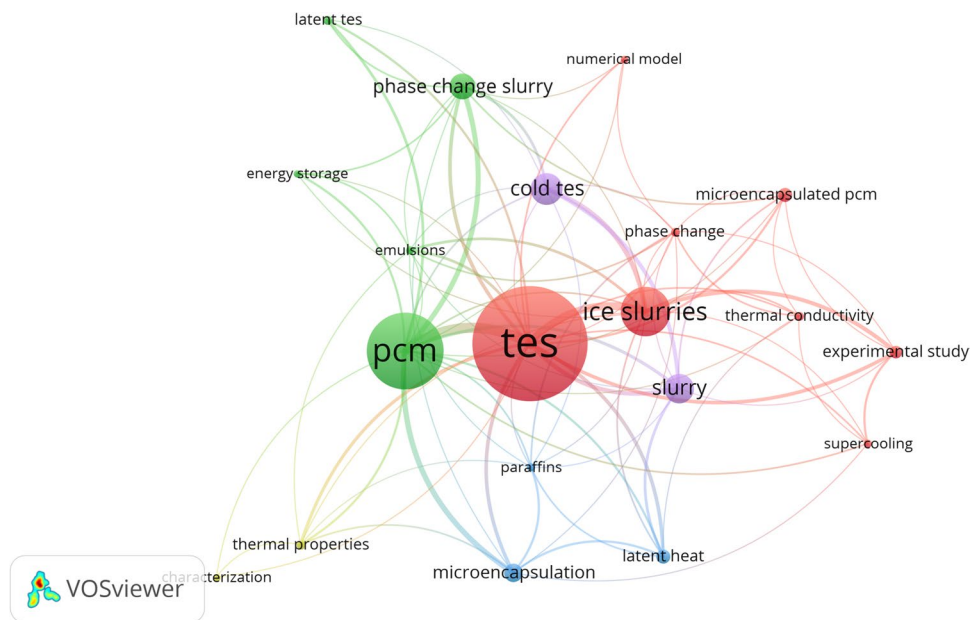


**Fig. 3** Co-occurrence of keywords elaborated with the software VOSviewer for slurries for TES applications



used was TITLE-ABS-KEY ("phase change material" OR "PCM") AND ("cold thermal storage" OR "cooling application\*" OR "cold storage") AND ("composite\*") AND NOT ("phase change memory" OR "porous carbon composites") AND (solar AND energy). Results shows that cold TES (yellow cluster) has a low relevance compared to other keywords. In this case a lot of studies were carried out at material level with nanomaterials (purple cluster) and in thermal management applications for batteries (blue cluster).

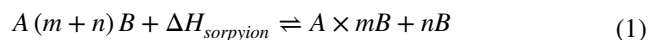
Figure 3 shows the co-occurrence of keywords elaborated with the software VOSviewer of the documents published until 2023 related to slurries for TES applications. Results were obtained Scopus database using the query TITLE-ABS-KEY ((thermal energy storage" OR "thermal storage") AND (slurr\*)) where it can be observed the main applications are related to cooling highlighted from the keywords "cold TES" and "ice slurries".

From the previous considerations, it is clear that there is an empty room in literature of works that sum up the behaviors of the composite materials, such as composite sorbents, slurries and composite PCMs, used for cooling and cold storage applications. These materials combine the favorable properties of different components to achieve superior cooling performance or higher cold storage capacity therefore, the authors provide an overview of composite materials, highlighting their advantages and recent advancements in the field. Specifically, the present paper addresses on: development and characterization of composite sorbents for refrigeration, air conditioning and cold storage systems, showing the investigations in terms of sorption properties, including adsorption/desorption

kinetics, equilibrium characteristics, and thermodynamic analysis. Formulation, preparation, and characterization of slurry-based cooling fluids for various thermal management applications. Design, synthesis, and characterization of composite PCMs incorporating nano/microencapsulated phase change materials within a matrix material, including the investigation of their thermal properties, phase change behavior, and thermal reliability under cyclic thermal loading conditions. Finally, it is highlighted that a big gap is still present in literature regarding the life-cycle/economic/environmental impacts of these families of materials.

## Sorbents

Adsorption cooling is a technology able to provide cooling exploiting low-grade heat sources (e.g. solar thermal, low-grade industrial waste heat) to drive the process instead of the mechanical energy commonly required by vapor compression chillers [4]. It exploits the ability of some solid sorbent materials to adsorb and desorb reversibly a vapor, depending on the temperature level applied to the sorbent material itself. In this case, the vapor represents the refrigerant of the adsorption cooling technology, and it is thermally compressed from the evaporator pressure up to the condenser pressure, thus allowing to complete the typical thermodynamic inverse cooling cycle employing only heat as driving source. The adsorption and desorption reactions are represented by the generic reaction below:



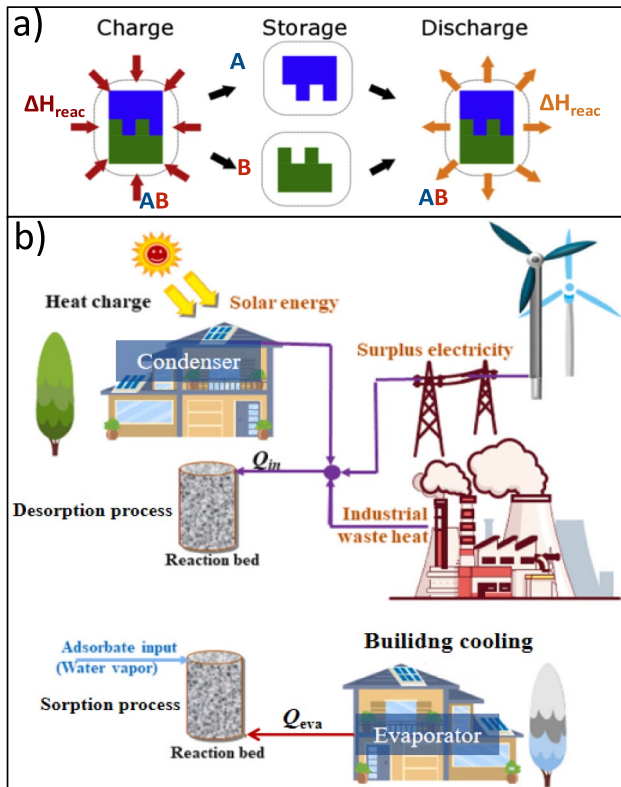


**Fig. 4** **a** The working principles and **b** operation process in buildings of adsorption cooling systems [5, 6]

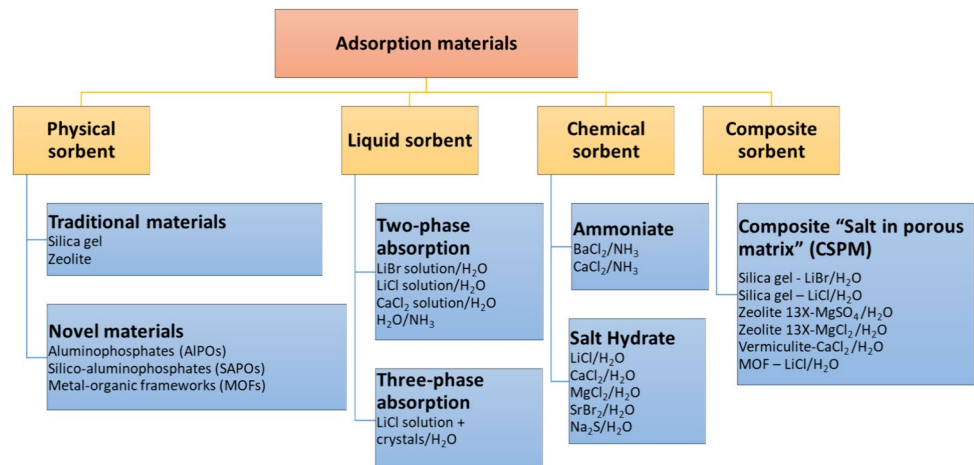
where A and B refer to the sorbent material and the vapor respectively. The vapor is often referred in the literature as sorbate. The related schematic of the process at material- and system-scale are represented is shown in Fig. 4a and b, respectively. During charging process, the renewable or industrial waste heat is used to regenerate the sorbents inside the reaction bed. In some cases, also the surplus of

renewable electricity can be converted into heat to drive the process. In this phase, the sorbate is separated from the sorbents and condenses in the separate vessel, the condenser. Thus, the heat is stored in the form of chemical bond, which can be stored with no heat loss by disconnecting the reaction bed from the condenser. When heating or cooling is needed, the evaporator is connected with the sorption bed, the sorbate from the evaporator is adsorbed by the dry sorbent. Meanwhile, the cooling effect is created at the evaporator where evaporation heat is needed to supply gaseous sorbate. The sorption heat released in the sorption bed is utilized if heating is needed. When the cycle is continuously operated, a sorption chiller/heat pump is obtained. On the contrary, when a long standby period occurs between desorption and adsorption phases, the system is operated as storage.

### Classification

The sorption-based systems work based on the interface between the sorbent and the gaseous sorbate. According to sorption mechanisms, the sorbents are classified into four categories [7]: liquid absorption, solid adsorbents, chemical reaction and composite materials, as shown in Fig. 5. Solid (physical) adsorption happens when the adsorbate ( $\text{H}_2\text{O}$ ,  $\text{NH}_3$ ,  $\text{CH}_3$ , etc.) is adsorbed in the vicinity of the sorbent surface and the inner pores driven by Van der Waals force [8]. The related sorbents are generally porous materials, like traditional silica gel, zeolite and activated carbon, and novel porous materials like aluminophosphates (AIPs), silico-aluminophosphates (SAPOs) and metal–organic frameworks (MOFs). Liquid absorption happens when the sorbate penetrates the surface of the liquid layer and enters the bulk body of the liquid. The general sorbates include  $\text{H}_2\text{O}$  and  $\text{NH}_3$ . The related solution consists of LiCl aqueous solution, LiBr aqueous solution,

**Fig. 5** The classification of sorption thermal energy storage materials. Adapted from [7]



etc. Especially, three-phase absorption was introduced by Yu et al. [9]. It can increase the total sorption amount by allowing the occurrence of crystals under controlled operating conditions. Chemical sorbents are characterized by chemical reactions with the adsorbate, the involved forces are intermolecular forces and chemical bonds. It generally consists of the hydration reaction between salt hydrates and water vapor and the coordination reaction of ammoniates. Porous materials have relatively thermal and structural stability, but the adsorption heat is the lowest (close to the evaporation heat); Chemical sorbents have the highest reaction heat, but it encounters problems of swelling and agglomeration after several working cycles.

To avoid such problems, Aristov et al. [10] proposed a novel composite “salt in porous matrix” (CSPM), made of porous matrix and salt hydrate. It can alleviate the swelling and agglomeration of the hydrated salt by dispersing them inside numerous meso- and micropores. A plenty of mass transfer pathway is supplied by the porous structure. The salt hydrates are dispersed inside the numerous pores, which contributes to greatly alleviating the swelling and agglomeration problems. Salt content is a critical parameter, a higher salt content can lead to larger water uptake but has poorer mass transfer efficiency. Additionally, there exists a maximum salt content to guarantee that the formed salt solution has a smaller volume than the pore volume, thus avoiding salt solution leaking out of the pores [11, 12].

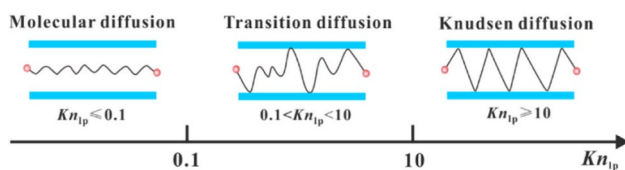


**Fig. 6** The classification of sorption thermal energy storage materials [7]

**Table 1** Texture parameters of typical physical sorbents reported in the literature

Adsorbents	BET surface area (m <sup>2</sup> /g)	Average pore diameter (Å)	Pore volume (cm <sup>3</sup> /g)	Refs.
Silica gel	Type RD	720	22	0.37 [16]
	Type A + +	863.6	22	0.47 [17]
	NS-10	586	27.8	0.41 [18]
Zeolite	AQSOA-Z01	189.6	11.78	0.07 [19]
	AQSOA-Z02	717.8	11.84	0.27 [20]
	AQSOA-Z05	187.1	11.76	0.07 [20]
Expanded vermiculite	0.671	7663.4	4.76	[12]
MOFs	UiO-66 (Zr)	1296.8	21.48	0.54 [21]
	Al-Fum	792.26	21.82	0.93 [22, 23]
	CPO-27(Ni)	299	7	0.22 [24]
	MIL-101(Cr)	3000–5900	30–34	1.80 – 2.00 [25, 26]

## Selection criteria

Sorption materials are the core part of the sorption-based systems, their selection criteria are as follows [13]:

- High massive or volumetric energy storage density.
- Low charging temperature.
- High sorption capacity.
- Large thermal conductivity and good heat and mass transfer.
- Non-toxicity, non-corrosiveness, and non-harmfulness to the environment and humans.
- Low cost.
- Good thermal stability and mechanical strength.

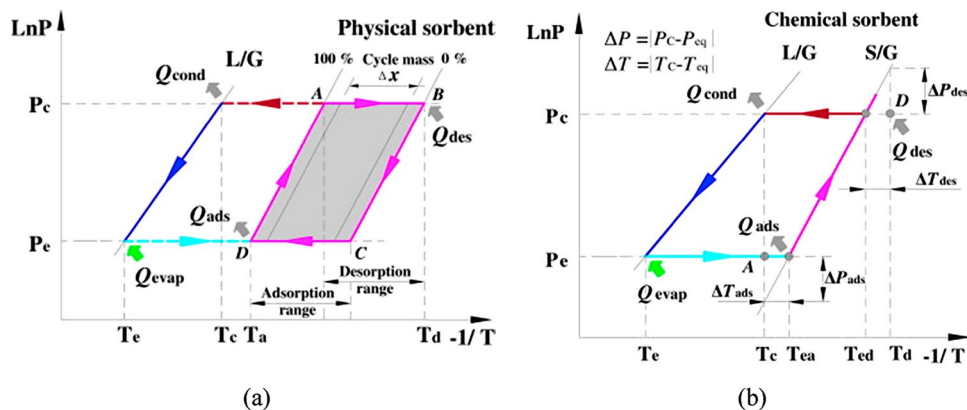
## Properties

The significant properties required to be measured and analyzed mainly include pore structure, sorption equilibrium, sorption kinetics, sorption heat and thermal conductivity.

## Pore morphology

It consists of pore distribution, specific surface area, pore volume and pore size. As discussed above, the adsorption of adsorbate inside the pores takes up most of the total sorption capacity, the pore volume decides the limitation of the maximum sorption amount. The porous materials can be classified into macroporous (pore diameter > 50 nm), microporous (pore diameter < 2 nm) and mesoporous (2 nm < pore diameter < 50 nm) materials. Different pore distribution and pore size contribute to different types of mass diffusion [14], as presented in Fig. 6.  $Kn_{ip}$  refers to the Knudsen number, defined as the ratio of the mean free path to pore diameter), when  $Kn_{ip} < 0.1$  molecular diffusion is established, transition diffusion when  $0.1 < Kn_{ip} < 10$  and Knudsen diffusion

**Fig. 7** Working cycles of: **a** Physical sorbents; **b** Chemical sorbents [27, 28]



when  $Kn_{ip} > 10$  [15]. The pore size influences the sorption energy, which generally increases with the reduction of the pore size. In addition, the pore volume and pore size are critical parameters that decide the selection of the inserted salt and the maximum amount of salt that can be inserted inside the pore volume.

Table 1 summarizes the pore parameters of some typical sorbents, including three types of silica gel, three types of zeolite, four types of MOFs and expanded vermiculite. Expanded vermiculite has macropores with a relatively large pore volume of  $4.76 \text{ cm}^3/\text{g}$ , it has negligible sorption ability, but it can contain a large amount of hydrated salts for the development of composites. Silica gel has mesopores with pore volume varying in the range of  $0.37\text{--}0.47 \text{ cm}^3/\text{g}$ . Zeolite has micropores, AQSOA-Z02 has a volume of  $0.27 \text{ cm}^3/\text{g}$  while AQSOA-Z01 and Z05 have relatively small pore volume. Among four types of MOFs, MIL-101(Cr) and Al-Fum have relatively large pore volumes.

### Sorption equilibrium

It is important to obtain and analyze the equilibrium sorption amount under various operation conditions, both for comparing the performances of different sorbents and

selecting proper sorbents aiming for different applications. For chemical sorbents, their solid–gas equilibrium line, namely, the relationship between the equilibrium pressure and temperature, can be described by Clausius–Clapeyron Equation:

$$\ln\left(\frac{p_{eq}}{p_0}\right) = -\frac{\Delta H_r^0}{RT_{eq}} + \frac{\Delta S_r^0}{R} \quad (2)$$

where  $p_{eq}$  and  $T_{eq}$  are equilibrium pressure and temperature, respectively.  $\Delta H_r^0$  and  $\Delta S_r^0$  are the standard enthalpy change and entropy change for the reaction, respectively. Different from chemical sorbents, the equilibrium sorption capacity of physical sorbents is determined by temperature and pressure altogether. In general, it increases with reduced temperature and increased pressure. Figure 7 (a) and (b) represented the working cycles of physical sorbents and chemical sorbents, respectively.

The Dubinin–Astakhov (D–A) equation is generally utilized to describe the equilibrium capacity under various operation conditions:

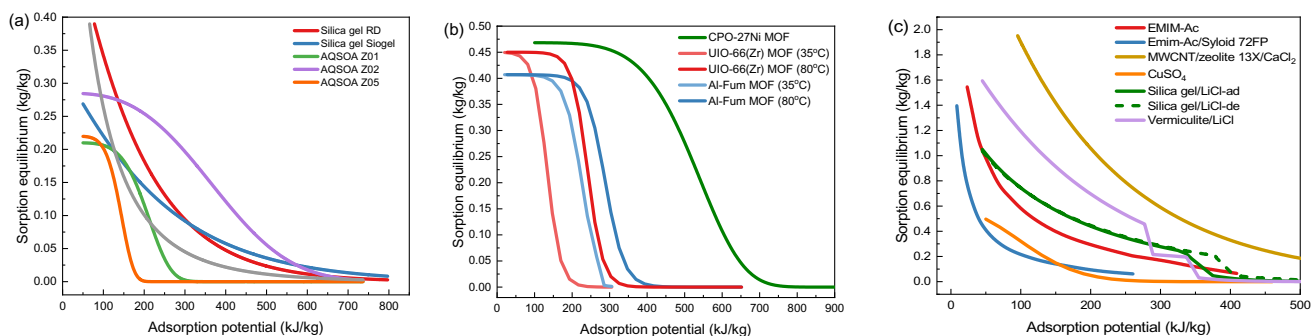


**Fig. 8** The changes of equilibrium water uptake of different types of adsorbents in the function of adsorption potential: **a** silica gel and zeolite; **b** MOFs; and **c**  $\text{CuSO}_4$  and composite sorbents

$$X_{eq} = X_0 \exp \left[ - \left( \frac{A}{E} \right)^n \right] \quad (3) \quad \left( \frac{\partial \ln P}{\partial T} \right)_v = - \frac{q_{st}}{RT^2} \quad (7)$$

where  $X_{eq}$  is the equilibrium uptake [kg/kg],  $X_0$  is the maximum sorption capacity based on the total accessible pore volume [kg/kg],  $E$  refers to characteristic energy [kJ/kg], and  $n$  means the empirical constant [-].  $A$  is the adsorption potential, which can represent the temperature and pressure:

$$A = RT \ln \frac{p_s}{p} \quad (4)$$

where  $R$  is the universal gas constant (8.314 J/(mol·K)),  $T$  is the adsorption/desorption temperature [K],  $p_s$  is the saturated vapor pressure at  $T$  [Pa], and  $p$  is the evaporation/condensation pressure [Pa].

Other sorption equilibrium models include the “S” shape isotherm model [29], Freundlich’s equation [30] and the Empirical fitting formula [31, 32]. Figure 8 shows changes of sorption equilibrium amount with the increasing adsorption potential. Generally, MOF can reach a higher sorption capacity than silica gel and zeolite, and composites obtain the highest sorption capacity.

### Sorption kinetics

Sorption equilibrium models give the maximum sorption amount that can be obtained, while sorption kinetics reflect the whole sorption process, and it influences the duration of the charging and discharging process and the design strategy of the reactors. Many kinetics models have been proposed, and the most utilized one is the Linear Driving Force (LDF) that is described by:

$$\frac{dx}{dt} = k(x_{eq} - x) \quad (5)$$

where  $k$  [s<sup>-1</sup>] is the kinetic parameter. This equation can be further transformed into:

$$x(t) = x_{eq}(1 - e^{-kt}) \quad (6)$$

where  $x(t)$  [kg/kg] is instantaneous uptake.

### Sorption heat

This parameter influences the required volume of reactor and the occupied area of the device, in case of sorption thermal energy storage operation. The adsorption enthalpy,  $q_{st}$  [J/mol<sub>sorbate</sub>] can be calculated by the isosteric heat obtained from the adsorption isosteres [33]:

The adsorption enthalpy can also be measured directly by calorimetric method, like using the simultaneous thermogravimetric-differential scanning calorimetry. Accordingly, the energy storage density can be calculated by:

$$\Delta H = - \frac{q_{st}}{M_g} [J/K] \quad (8)$$

where  $M_g$  [g/mol] is molar mass of the sorbate, and  $w$  [g<sub>sorbate</sub>/g<sub>sorbent</sub>] is specific adsorption amount.

### Thermal conductivity

The efficient heat transfer between the reactor and the heat transfer fluid is critical for releasing good-performance practical devices. The main heat transfer processes consist of the heat conductivity of the inner and between the sorbent particles and the convection heat transfer between the sorbents and heat transfer fluid. Generally, the heat conductivity of sorbents is lower than 0.5 W/m/K, which is not favorable for sufficient heat transfer. To enhance the heat transfer of the sorbents, enhancing heat transfer materials (like expanded natural graphite) were utilized to be combined with the sorbents. Yu et al. [34] developed a new type of consolidated sorbents, by mixing activated carbon-LiCl composite with expanded natural graphite treated with sulfuric acid (ENG-TSA) with silica solution serving as the binder. The obtained consolidated has a much higher thermal conductivity (2.83 W/m/K) than the bulk activated carbon-LiCl composite (0.14 W/m/K).

### Phase change materials (PCM)

Latent heat storage allows to use the thermal energy of different sources (e.g., sun, industry waste heat, ovens, etc.) when it is required or in the absence of the specific warm source, employing different materials during the phase transitions which are known as phase change materials (PCMs) [35].

The desired temperature range of application is determining for the selection of the PCM, which can be categorized according to this aim in low, medium, and high temperature PCM. However, the practical application of this kind of substance can be hindered by challenges such as flammability, low thermal conductivity, phase segregation, subcooling, corrosion, thermal degradation, among other difficulties. In this regard, PCM can be modified to enhance their thermal and physical behavior,

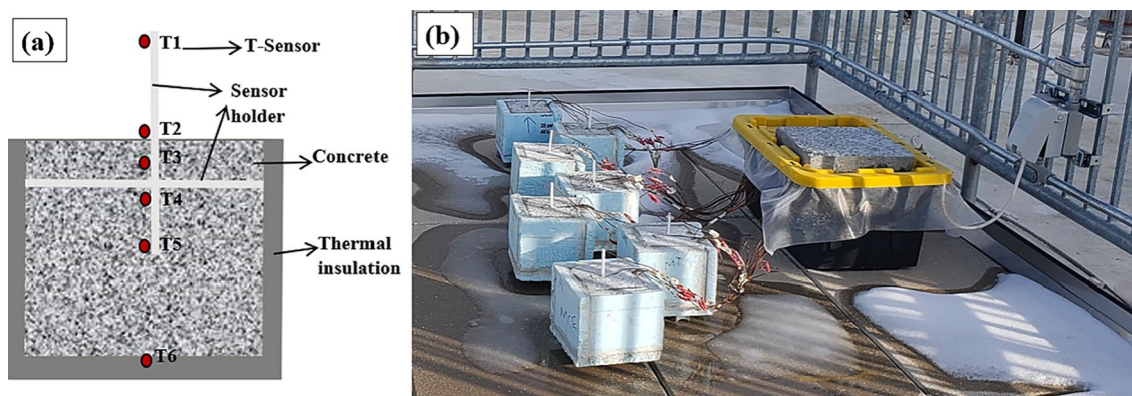


**Fig. 9** Concrete samples set-up: (a) t-wire sensors and thermal insulation, and (b) winter field test [40]

and one of the most successful modification technologies is the encapsulation of the PCM, which could be classified according to the design of the material in core–shell materials and shape-stabilized PCMs (SS-PCMs) [36]. Another way is by adding different compounds acting as nucleating agent [37] and/or thickening agents [38]. Even hybrid methods were employed to enhance the TES systems, like composites including porous media and fin, nanoparticle and fin, encapsulation and porous media, as support materials, among others [39]. In general, SS-PCMs and PCM modified with different agents can be considered as composite phase change materials (CPCMs); consequently, CPCMs seeks for the enhancement of the thermal and/or physical properties of PCM for specific applications like different cooling systems for thermal management of building, photovoltaic systems, batteries, and electronic devices.

Due to the relatively low provision and abundance of PCMs solidifying at low temperature (below 40 °C), the knowledge and evaluation of the type of CPCMs, their selection criteria, and the different properties that should be determined and analyzed are fundamental for the development of new CPCMs and their possible applications in real life. An important factor is their abundance and cost, that is why natural and waste products are being proposed for CPCMs. For example, a CPCM conformed by blends of soybean oil, coconut oil, and paraffin wax were coated by latex for building thermal regulation by the use of CPCM modified concrete (Fig. 9), which contribute with both sensible and latent heat storage [40]. In addition, bischofite as a by-product of the non-metallic mining industry, has been analyzed as CPCMs mixed with polyethylene glycol (PEG) (to improve its thermal behavior) [38], graphite (to improve its thermal conductivity), with excellent results.

Later, graphite flakes were employed to prepare a CPCM based on expanded graphite (graphite matrix/41.3 wt.% bischofite + 58.7 wt.%  $\text{Mg}(\text{NO}_3)_2 \cdot 6\text{H}_2\text{O}$ ) by mixing

the flakes with an intercalation agent followed by high temperature shock treatment, with a worm-like structure presenting numerous pores of different diameters. Moreover, the typical high volume change during melting/crystallization of most of PCM does not occur for the inorganic CPCM; contrary, it was demonstrated that for this CPCM a slight contraction after reaching the melting point occurred (around 4.5% for the “through-plane” orientation sample) (Fig. 10) [41].

### Classification of PCM

The nature of the compounds forming the PCMs is the main factor to establish a classification of PCMs (Fig. 11) but is not an exclusive factor. The PCMs can be as well categorized depending on the modification of the initial material in core–shell encapsulated PCM or form-stable PCMs (known also as shape-stabilized PCMs: SS-PCMs). In addition, depending on the attributes of the encapsulating material it could be specified as macro-, micro- or nano-materials. All these categories should be considered when selecting a PCM, and there are other factors to consider which will be discussed in the next section.

### Selection criteria of PCM

Different selection criteria have been presented across the decades and the most relevant is the phase transition point since the potential application will depend on it, as well as the latent heat, which allow to estimate the amount of heat stored during phase transition.

Specifically, the temperature range between the CPCM and the source/application determine the charging/discharging power of the system, and a high latent heat will be crucial to reduce the volume of the store along with the density [43]. However, there are several other factors which must be considered when selecting a composite



**Fig. 10** Representation and parameters of through-plane (TP) graphite matrix (right) and expansion curves for TP graphite orientation for different CPCM, including bischofite composite (left) [41]

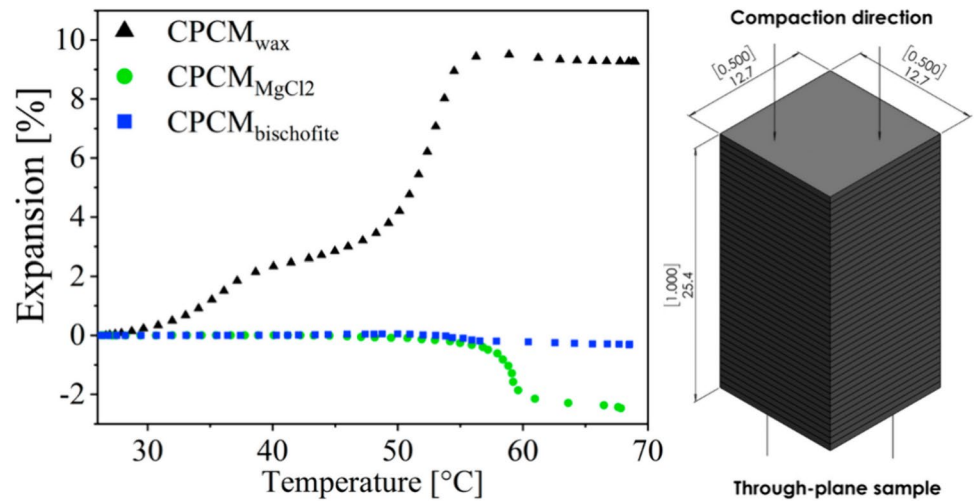


**Fig. 11** General categories for the different PCMs due to nature and phase transition. Adapted from [42]

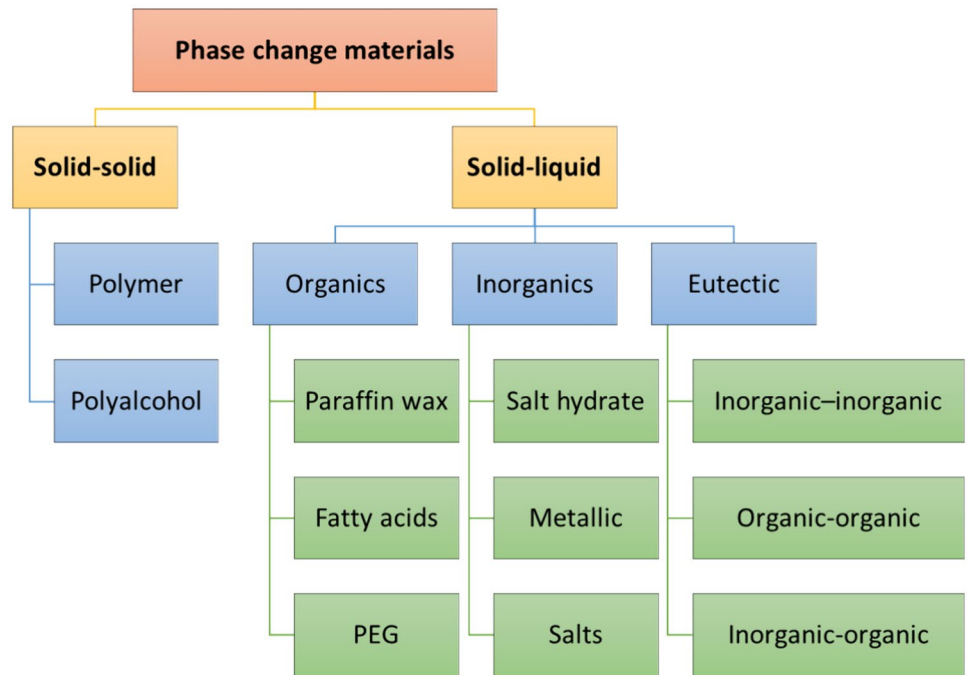


**Fig. 12** Importance of selection criteria

as PCM (Fig. 12). The compatibility between the different component of the formulated CPCM and with the encapsulation or container material (support material) is essential to avoid corrosion, degradation, and leakage, as well as to guarantee mechanical performance, especially when inorganic materials are in contact with metals and when plastics are employed to hold organic PCMs, like

paraffin. Thermal, physical, and chemical stability should be expected after several cycles. A high thermal conductivity should be provided when applications require high discharging power, therefore numerous research are focused to enhance this parameter. Finally, the abundance of the selected materials should be high and the costs as low as possible, that is why the use of wastes or natural

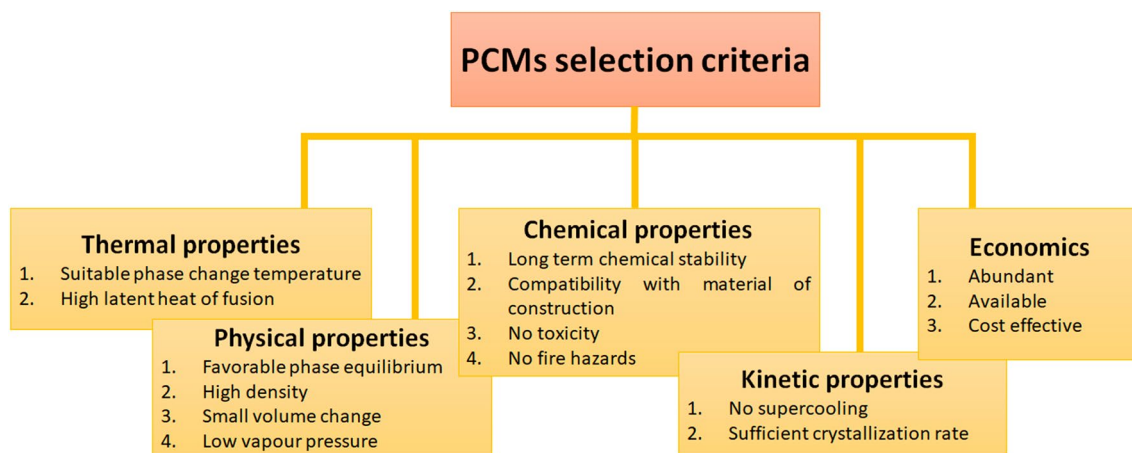


**Fig. 13** Various parameters used in the selection of PCM (adapted from [42] and [47])

products and by-products as PCM or the additive materials have been frequently proposed [44]. In this sense, the use of waste materials and by-products from mining industry and minerals as candidates for PCMs or as their components for CPCM formulations could greatly support in lowering the total cost of the storage system with an additional environmental and social impact like decreasing greenhouse emissions and diminishing the landfilled waste amounts [45, 46]. A most detailed criteria selection

was provided by Singh and collaborators [47] (Fig. 13) including kinetic and economic factors. Additionally, a recent strategy for PCM ranking was proposed by M. Awan and co-authors [48] and involves three main steps: including model development, performance testing and results verification.

**Table 2** Some essential properties and measurement methods that allow demonstrating the performance and applicability of CPCMs

Properties	Abbreviation	Units [53]	Methodologies	Observations
Phase change temperature	$T_m, T_c$ or $T_s$	$^{\circ}\text{C}, \text{K}$	Thermogravimetric analysis (TGA), Differential scanning calorimetry (DSC), and/or Simultaneous Thermal Analysis (STA)	The initial point where the first amount initiates the phase change process
Latent heat or enthalpy	$L, \Delta H,$ or $h$	$\text{J/g}, \text{kJ/kg}$		The area under the curve during the phase change process
Heat capacity	$C_p$	$\text{kJ}/(\text{kg}\cdot\text{K})$		
Thermal stability		Degradation reactions		Described according to the weight losses and the heat performance
Subcooling degree	$\text{SC}$ or $\Delta T$	$^{\circ}\text{C}$		Difference among the fusion and the solidifying points
Cycle stability		Number of cycles		The deviation of the first latent heat and that of the last heating/cooling cycle is a way to determine this factor
Energy storage density	$\text{esd}$ or $\text{e.s.d}$		Estimated employing $L$ and the density $\rho$ of the material	The complexity of density estimations inhibits its determination
Thermal conductivity	$\lambda$	$\text{W}/(\text{m}\cdot\text{K})$	Several techniques and equipment, e.g., Transient Plane Source Method employing a TPS 2500 S equipment from Hot Disk AB [54, 55] employing a NETZSCH LFA 467 laser thermal conductivity meter [56], a C-THERM Instrument [57], among others	The results are generally provided employing a correlation among the $\lambda$ of pure PCM and the CPCM
Leakage			Determined by visual comparative melting test	Appearance of liquid out the CPMs shows leakage problems

**Table 3** Several of the most recent composite PCMs for cooling in buildings published in the last two years

PCM classification	PCMs	Composite	PCM mass fraction (wt.%)	Preparation method	Melting point (°C)	Solidification point (°C)	Latent heat (J/g)	Refs.
Organic	Paraffin wax	Corn straw	99.7	Vacuum impregnation	54.6	37.2	186.0	[58]
		Carboxylated Cellulose			36.5	32.2	130.6	[59]
		nano crystals/ Palygorskite/ Portland cement/ Zeolite/River sand			41.3	40.1	61.5–65.7	[60]
	Lauric acid (99% pure) and Myristic acid (98% pure)				66.9–71.1	28.8–33.8	173.0–185.5	[61]
	Polyethylene glycol (PEG)-6000	Few-layer graphene (FLG) and Melamine foam (MFs)	MF@PEG-5, MF@FLG/PEG-5, and MF@FLG/PEG-10		60.9–63.1	39.6–43.2	126.0–166.0	[62]
		Delignified wood (DW)/polyethyleneimine–boron nitride layers	PW2@PEG, PW5@PEG, PW10@PEG and PW15@PEG		54.2	31.4	50.5	[56]
	PEG-4000	Steel slag	35		60.0 65.0	21.0 – 30.0	125.3	[63]
	polyethylene glycol (PEG)	Reduced graphene oxide (rGO)	37–65		133.0–141.0	30.0–36.0	280.7	
	erythritol (ET)	nanosheets decorated with Ni nanoparticles	52–71					
	Several RUBITHERM paraffin	Gypsum, biochar and lignin	Several		24.0 – 34.0	16.0–26.0	83.0 – 88.0	[54]
Inorganic	Octadecane	Porous aluminum nitride			26.0	25.0	116.3	[64]
	PEG 2000	Layered cellulose/ Fe <sub>3</sub> O <sub>4</sub> skeleton	95.3	Melting-impregnation	56.7	28.8	172.6	[65]
	Na <sub>2</sub> CO <sub>3</sub> ·10H <sub>2</sub> O; Na <sub>2</sub> HPO <sub>4</sub> ·12H <sub>2</sub> O	Rice husks	90		34.0	–	158.9	[66]
	Na <sub>2</sub> SO <sub>4</sub> ·10H <sub>2</sub> O	Na <sub>2</sub> SO <sub>4</sub> ·10H <sub>2</sub> O; NH <sub>4</sub> Cl; KCl; Na <sub>2</sub> B <sub>4</sub> O <sub>7</sub> ·10H <sub>2</sub> O; (C <sub>3</sub> H <sub>3</sub> NaO <sub>2</sub> ) <sub>n</sub>	Different proportions		7.1–13.4	5.1–12.9	128.4–143.3	[67]
	CaCl <sub>2</sub> ·Mg(NO <sub>3</sub> ) <sub>2</sub> ·6H <sub>2</sub> O (6%)	Fumed silica/ strontium chloride hexahydrate	97.5		21.3	27.5	142.4	[68]

Those works that appear in the green rows employed natural products as raw material for the formulation of the respective composites

**Table 4** Some of the most recent organic composite PCMs for cooling in different thermal management systems published in the last two years

PCMs	Composite matrix	PCM (wt.%)	Preparation method	Melting point (°C)	Solidification point (°C)	Latent heat (J/g)	Application	Refs.
PEG-6000	Nickel-plated melamine sponge/ MXene(Ti <sub>3</sub> C <sub>2</sub> T <sub>x</sub> )	98	Vacuum impregnation and sol-gel process	63.0	38.9	154.3	Heat dissipation within electronic devices and electromagnetic interference shielding	[50]
PEG	Polyvinyl butyral/graphene nanoplates	80	Melt blending	58.8	38.8	147.8	Adjustment of the working temperature of photovoltaic cells and improve its photovoltaic conversion efficiency	[49]
Paraffin wax	Stearic acid-grafted bisphenol A and porous expanded graphite network impregnated with alkylated boron nitride	–	Mixing, hot-pressing, and injection molding	–	36.0 and 37.0	93.5	Heat dissipation within electronic devices heat dissipation within electronic devices	[69]
Lauric acid	Reduced graphene oxide aerogel/silver nanowires	95.4	Melt blending and physical insertion of nanowires	–	–	185.8		[70]
Pristine paraffin	Copper foam	Saturated	Melting impregnation	30.0	–	138.9	Passive cooling of a heat source form a thermoelectric generation system	[71]
SP31	Copper oxide and aluminum oxide hybrid nanoparticles	–	Melt blending	29.0 – 31.0	–	200.0	Thermal management of photovoltaic solar cell	[72]
Oleic acid and beeswax	Metal matrix sheets		Melt blending and physical insertion of sheets	37.6		141.0	Thermal management of photovoltaic solar cell	[51]
Paraffin	Carbon nanotube/boron nitride/silicone gel	40	Spray drying technology and cool vacuum mixing and vacuum impregnation at room temperature	54.8	–	133.0	Lithium-ion batteries (LIB) thermal management	[73]
	Graphite	–	Manufactured by Wuhan Saimo New Energy Technology Co., Ltd	40.0	–	230.0		[74]
	Styrene ethylene butene styrene block copolymer/expanded graphite phase/change polymer skeleton synthesized from polyethylene glycol	80.8	Polycondensation reaction and melt blending	40.8	–	221.3		[75]
n-Docosane	Expanded graphite/copper nanoparticle	83.3	Melt blending and ultrasonic assisted mechanical stirring	43.9	42.0	205.0		[76]

Those works that appear in the green rows employed natural products as raw material for the formulation of the respective composites

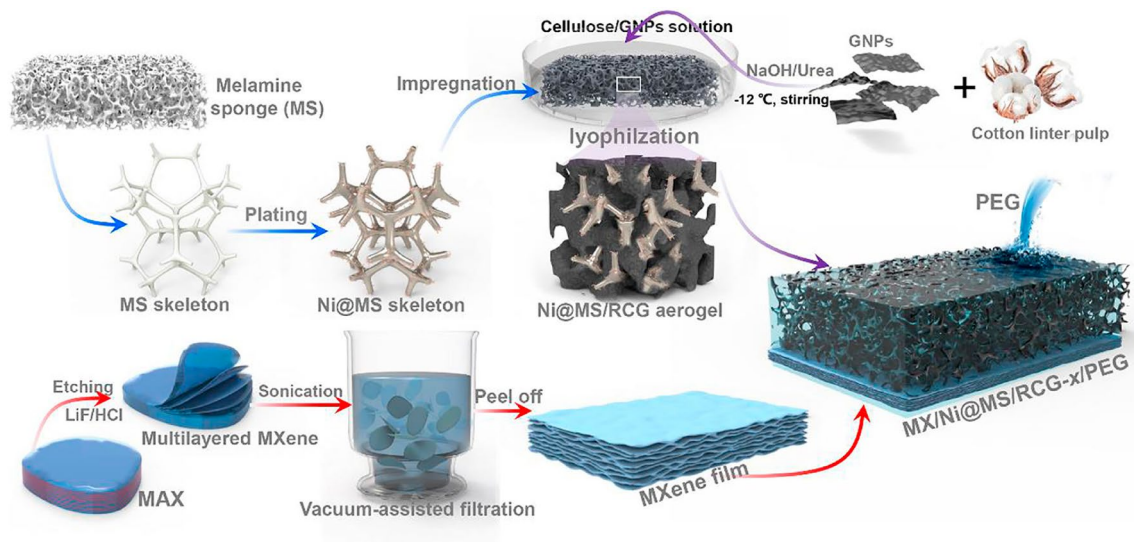
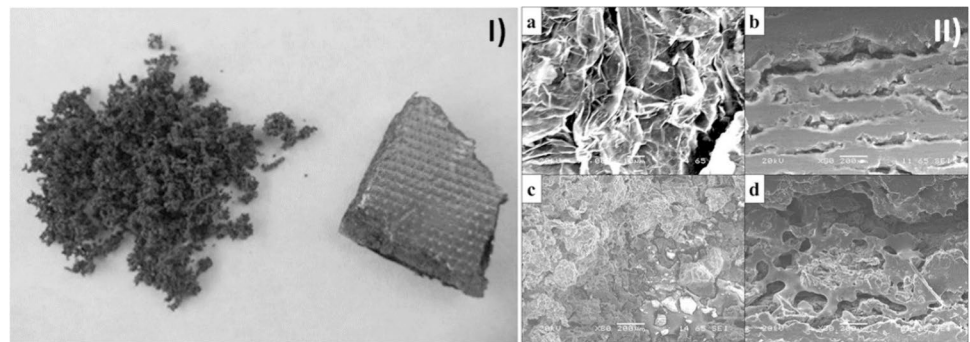


**Fig. 14** Formulation process of MX/Ni@MS/RCG-x/PEG composite PCMs [50]

**Fig. 15** (I) Expanded graphite matrix (right) and flakes (left) and (II) SEM images of (a) EG flakes, (b) EG matrix, and CPCM based on inorganic mixture and 5wt.% of EG flakes (c) and 5wt.% of EG matrix (d) [80]



## Formulation methods

Once selected the desired materials, is time to develop the new CPCM, and there are some approaches to perform these formulations. First, it is important to determine the thermal characteristic of all components involved, since almost all methods include the melting process of the PCM, consequently is established which component will remain at solid state and which will melt along the PCM. Considering this, if two or more components of the CPCM formulation will be melting together then the methodology will follow the “melting blending” path [49]; otherwise, if only the PCM is melted at the working temperature and the rest or the main component remains at solid state there are three paths: “melting impregnation”, “vacuum impregnation” [50], and “physical blending” [51] methods (see Table 2, Table 3 and Table 4). In addition, during formulation of CPCM parameters as the nature and amount of the employed dissolvent and reactants should be evaluated, since final thermal properties of CPCMs and porosity of support materials depend on the final media achieved during the formulation [52].

Eventually, those are not the only available technologies. PCMs can be embedded directly into building materials like gypsum boards [77, 78] or into shaped porous micro or nanomaterials (e.g., polygorskite microspheres composites) [59] which could be incorporated into walls and roof decreasing energy consumption around 50% of total consumption under the absence of PCM [79]. Even more complex formulations are being recently developed employing several methods at once; e.g., Cheng et al. [50] prepared a MXene film by vacuum-assisted filtration process to develop a new shape-stabilized MXene/Ni-plated melamine sponge/Regenerated cellulose/Graphene nanoplate/Polyethylene glycol CPCM via sol-gel and electroless plating methods (Fig. 14).

Ultrasonic assisted impregnation improves the homogeneity of the mixtures providing a material with better cycle stability and avoiding leakage due to low impregnation efficiency. However, ultrasonic impregnation procedure is longer respect to the vacuum impregnation method [80]. This result was provided during the formulation of a CPCM composed by a mixture of 40 wt.%

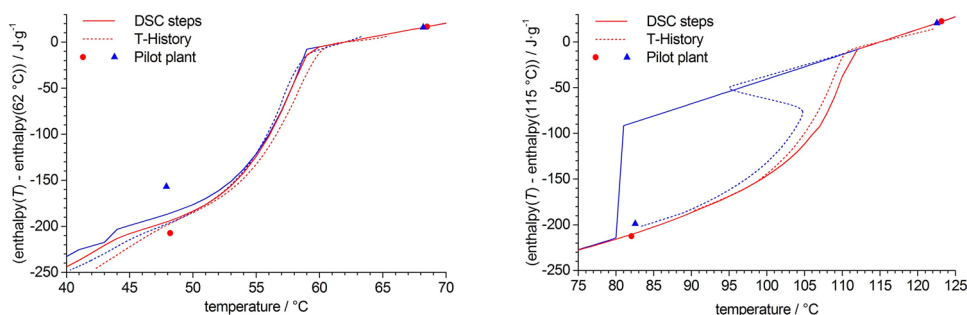


**Fig. 16** Enthalpy curves of RT58 (left) and bischofite (right) measured via DSC in step mode (solid line) and T-History (dashed line). Red circles and blue triangles indicate the enthalpy changes measured at pilot plant scale upon melting and crystallization, respectively [83].

$\text{MgCl}_2 \cdot 6\text{H}_2\text{O}$  and 60 wt.%  $\text{Mg}(\text{NO}_3)_2 \cdot 6\text{H}_2\text{O}$  impregnated into two expanded graphite flakes and expanded graphite matrix (Fig. 15), where the optimal encapsulation efficiency was achieved after 1 and 3 h employing vacuum and ultrasonic impregnation, respectively, with a decrease in subcooling degree and an expected high enhancement in thermal conductivity (reflected in a decrease on melting time) [80].

## Properties

Pursuing an effective implementation of the CPCMC technology, a previous accurate characterization is essential to demonstrate a satisfactory thermal performance. Thermophysical properties are those which give information about not only the amount of energy that PCMs and composites can store and the phase change temperature, but others which will reveal practical issues and reliable pertinence, like thermal conductivity, energy density storage, and thermal and cyclic stabilities. In Table 2, the most important parameters and methodologies are presented. In addition, analyzing how these parameters change due to the addition of the different components of the CPCMC could be revealing.

### Melting and solidifying temperatures

Selection of a suitable PCM for a specific application requires that the whole phase change process takes place within the temperature range of this application; it means, within the range of charging and discharging temperature of the proposed application. Formulations of CPCMC are delivered to enhance one or more drawbacks of the pure PCM but is a fact that it alters the charging-discharging range of the final material. Consequently, this variation should be considered always, even it is slight, as usually occurs; since

The enthalpy curves measured via DSC and T-History indicate a volume-independent melting and crystallization behavior of the PCMs, and the number of steps in which these melting/solidification process occur

later when the composite is included in a heat storage system, this variation could be potentiated by other factors like the orientation on thermal transport [81] or the heights of the CPCMC packing bed [67]. In addition, different aspects are also related with this variation on phase change temperatures, for instance, the contact due to hydrogen bonding or capillary forces among the PCM and other components in the final composite [82], or caused by a limiting effect of the porous structure over the PCM [63].

### Latent heat

The enthalpy change or latent heat is directly related to the storage capacity of a PCM in a specified temperature range [83]. It can be determined by differential scanning calorimetry (DSC), thermogravimetric analysis (TGA) or related techniques, and t-history methods; and expressed mainly in  $\text{J/g}$  or  $\text{kJ/kg}$  (Table 2 and Table 3). The value of pure PCM is affected when PCM is immersed in CPCMCs, since the other components of the final material generally do not contribute to heat storage. For example, an erythritol based CPCMC, with a complex support achieved with nickel foam skeletons filled with reduced graphene oxide nanosheets adorned with Ni nanoparticles, showed  $280.7 \text{ J/g}$  (see Table 3), which is lower in comparison with pure erythritol ( $349.0 \text{ J/g}$ ), but CPCMC allowed to stop leakage problems [63]. Moreover, differences in enthalpy values among composites is assigned mainly due to variation in PCM loading (%). Comparing organic with inorganic CPCMCs (Table 3), it was observed that in first ones had the higher latent heat values, meanwhile latent heat above  $120 \text{ J/g}$  were achieved by all reported inorganic CPCMCs.

For the implementation of a new CPCMC in real applications, thermal performance studies of latent heat storage at pilot plant scale are necessities, which can be performed employing temperature sensors. The analysis of this latent heat measurements should be performed by the tabular

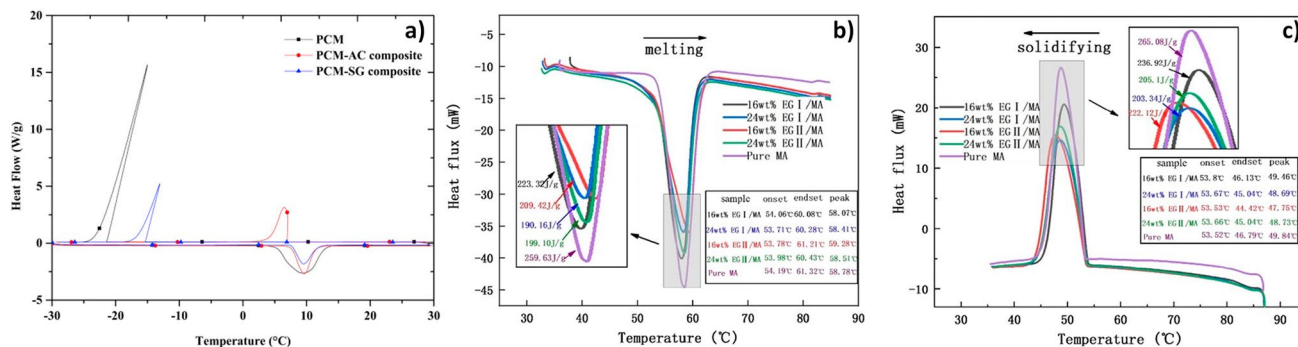
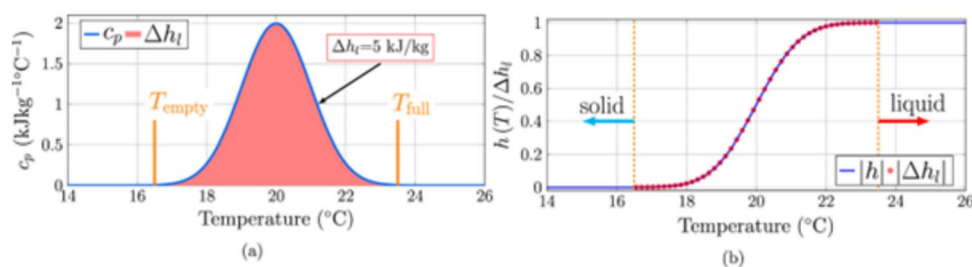


**Fig. 17** Different representations of subcooling degree determined by DSC technique. **a**—Pure PCM OM-11 and composites with activated charcoal (PCM-AC) and silica-gel (PCM-SG) [86], **b**—pure myris-

tic acid (MA) and **c**—MA—expanded graphite (EG) shape-stable CPCMs [87]

**Fig. 18** **a** Specific heat–temperature curve defined by a normal probability density function. **b** Integral of the specific heat–temperature curve divided by the specific latent heat



enthalpy changes or by enthalpy–temperature plots within designated temperature ranges. However, at different scale and under different conditions, the latent heat could result distinct for each method, the enthalpy–temperature plots (Fig. 16) were demonstrated to be profitable [83].

### Subcooling degree

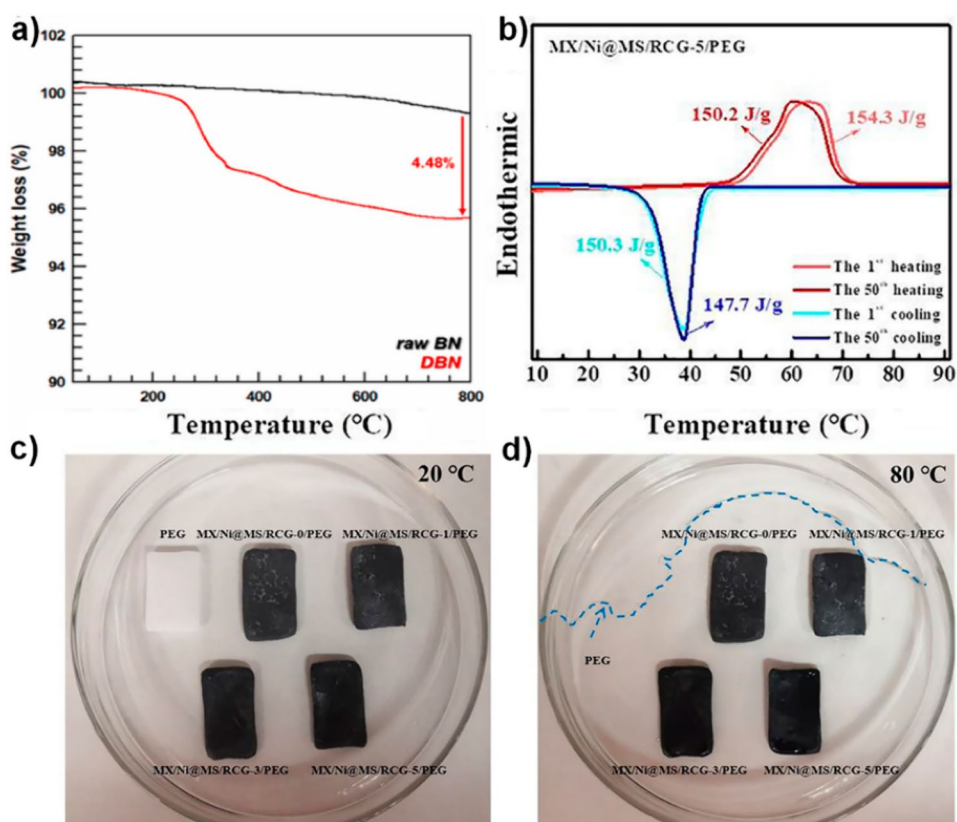
Subcooling, undercooling, or supercooling are terms related to the phenomenon of a substance which remains liquid several degrees under its solidification melting point; hence, the subcooling degree (SC) is the temperature difference between the melting point and the real temperature in which it solidifies. This phenomenon leads to a detriment of the stored heat, altering the cooling performance and thus the cycle life of the composite [67]. Different methods, like mechanical agitation, the addition of nucleating agents, chemical modifications, and the encapsulation of the PCMs were employed to reduce or eliminate subcooling degree, including the formulation of CCPM [84].

Normally, organic PCMs do not show this phenomenon or show a low SC (below 4 °C). Contradictory, inorganic PCMs usually show high SC degrees reaching values as high as 40 °C. Since the supercooling degree depends on melting and solidification temperatures, the methods to determine this parameter are those employed for phase change points and latent heat, mainly DSC, TGA and t-History. This

factor depends on the material nature, size and purity [85]; therefore, it is affected by the composition and nature of the final CPCM. In general, a decrease on subcooling degree is expected when formulating a CPCM. However, this is not always the case, for example, a composite was designed employing OM-11 (with a subcooling degree around 24 °C) as PCM and charcoal/silica gel particles as support material, achieving a reduction only around 7.0 °C, which is insignificant when compares to the achieved by OM-11 – activated charcoal composite (with a final subcooling degree around 3 °C, Fig. 17a) [86].

Recently, myristic acid (MA) and expanded graphite (EG) were employed for shaped CPCMs with different ratios, obtained by melt blending–press forming method, resulting in a decrease on the supercooling degree (Fig. 17b and c). The authors explained that heat transfer enhancement due to the support material and the heterogeneous nucleation helped the phase change of MA, reducing the distance among the melting and solidifying points [87]. Similarly, solid waste steel slag was applied with polyethylene glycol (PEG) for low temperature applications achieving a reduction on subcooling degrees under 5 °C (where PEG subcooling degree around 25 °C) [56]. Finally, the formulation of CPCMs is not the only path to reduce subcooling degree, another way probed by Wang et al. was preheating the CPCM prior to operation, due to the freeze–thaw cycle.

**Fig. 19** **a** TGA curves of raw boron nitride (BN) and prepared alkylated BN (DBN) [69]; **b** DSC curves of Ni@MS/RCG-5/PEG after 50th thermal cycles; **c** and **d** photographs of different samples on the hot stage of different temperatures [50]



### Heat capacity

In a storage unit, thermal energy storage capacity for charging ( $Q_{\text{charging process}}$ ) and discharging ( $Q_{\text{discharging process}}$ ) processes can be acquired as [88, 89]:

$$Q_{\text{charging processes}} = \int_{T_{H\text{-out}}}^{T_{H\text{-in}}} \rho \nu C_p T dt \quad (9)$$

and

$$Q_{\text{discharging processes}} = \int_{T_{C\text{-in}}}^{T_{C\text{-out}}} \rho \nu C_p T dt \quad (10)$$

where  $T_{H\text{-IN}}$ ,  $T_{H\text{-OUT}}$ ,  $T_{C\text{-IN}}$ ,  $T_{C\text{-OUT}}$  are the temperatures of the inlet hot heat thermal fluid (HTF), the outlet hot HTF, the inlet cold HTF, and the outlet cold HTF, respectively;  $\rho$  is the density ( $\text{kg}/\text{m}^3$ ),  $\nu$  is the volume flow rate ( $\text{m}^3/\text{s}$ ), and  $C_p$  is the specific heat capacity ( $\text{J}/(\text{kg}\cdot\text{K})$ ).

Sensible heat storage (SHS) is the storage mechanism which is well defined by heat capacity, according to the mass of the material and the temperature range, while during latent heat storage this property do not apport to the energy saving process [90]. However, it is important to analyze how CPCMs store heat first by SHS before the phase change process. Hence, the total stored energy is the sum of sensible

heat (before and after the phase change process) and latent heat stored in a specified temperature interval.

Specific heat capacity  $C_p$  is a very important parameter for numerical analyses, whereas many thermal variables as possible must be known. An accurate estimation of the state-of-charge was provided for cooling applications based on a non-linear state observer, which employed the thermophysical properties, including  $C_p$  and latent heat (Fig. 18), of the storage medium and the HTF in a simple one-dimensional dynamic model [91]. In addition,  $C_p$  was also employed to determine other parameters as thermal conductivity, e.g., the thermal conductivity ( $\lambda$ ) of a composite based on bischofite and expanded graphite for LiBs management was estimated by a Xenon Light Flash Diffusivity Analyzer (for thermal diffusivity  $\alpha$  determination) according to  $\lambda = \alpha \cdot \rho \cdot C_p$  [41]

$$\alpha = \frac{\lambda}{\rho \cdot C_p} \quad (11)$$

Recently, the addition of copper foam fins to a vertical shell-and-tube latent thermal energy storage unit successfully improved not only the heat exchange capacity of the systems, but the performance of the paraffin employed as PCM (RT-55) [89].



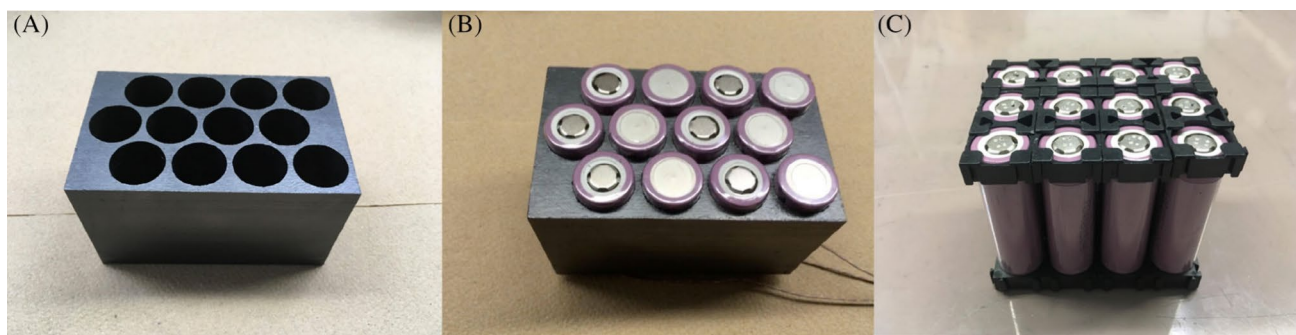


**Fig. 20** Assembly of the battery packs: **A** expanded graphite matrix impregnated with PCM (CPCM); **B** CPCM with Li-ion cells inserted **C** reference pack with no CPCM [39]

### Energy storage density

The potential application of new materials, also requires the assessment of energy storage density (e.s.d.) [92], which is the amount of heat (MJ) that can be stored in  $1 \text{ m}^3$  of material, and can be calculated according to [93]:

$$e.s.d. = \rho \cdot Q \quad (12)$$

where  $Q$  is the amount of stored heat, and can include both, sensible heat, and latent heat. The e.s.d. indicates the amount of energy stored by volume of material, which is a relevant indicator to compare among CPCMs, hence is here encouraged to report in all scientific works. Yang and co-authors [63] developed several Nickel foam/Ni nanoparticles – reduced graphene oxide / erythrol composites, employing e.s.d. as the selection criteria reaching a value around  $280.66 \text{ J/g}$ . However, among the reported works, almost none of them include the evaluation of e.s.d., mainly due to the complexity of determining the density of the final composite. Consequently, it was reported another way to visualize e.s.d., which is related to the ratio of latent heat between the composite and pure PCM; denoting a high e.s.d. value when is closed to 100% ( $\Delta H_{\text{CPM}}/\Delta H_{\text{PCM}}$ ) [94].

### Thermal and cycle stabilities

Thermal stability is that point at which PCM starts thermal and chemical decomposition or degradation, and can be determined by TGA, STA or related techniques. It is expected that PCM starts degrading first than the support material (which should occur far from the temperature range of desired application). A new CPCM comprising stearic acid-grafted bisphenol A and paraffin into a porous expanded graphite matrix infused with alkylated boron nitride ( $93.5 \text{ J/g}$ ) showed elevated thermal stability up to  $150 \text{ }^\circ\text{C}$  (Fig. 19a), with no leakage or degradation; for

advanced electronic packaging under  $90 \text{ }^\circ\text{C}$ , with a difference of  $60 \text{ }^\circ\text{C}$  between the desired application temperature range and its thermal stability [69].

The cyclic DSC characterization of shape-stabilized MXene/Ni-plated melamine sponge/Regenerated cellulose/Graphene nanoplate/Polyethylene glycol CPCMs (Ni@MS/RCG-5/PEG) (Fig. 19b) indicated a latent heat of  $150.2 \text{ J/g}$  and  $147.7 \text{ J/g}$  for melting and crystallization, respectively, even after 50 cycles, promising a long term use [48].

Shape stability is another factor which helps avoiding colossal leakage of molten PCM during heating/cooling processes. The formulation of CPCM allow to retain the melted PCM by capillary force and synergistic effects [36, 50]. It can be observed how polyethylene glycol based CPCM does not present leakage after melting at  $80 \text{ }^\circ\text{C}$  (Fig. 19c, d).

### Thermal conductivity

Thermal conductivity ( $\lambda$  or  $k$ ) of PCM is closed related to the store of thermal energy during phase change processes, the lower the thermal conductivity of the PCM the higher the time for storing heat. Inorganic PCMs presented higher thermal conductivities than the organic PCMs, specially for salt hydrates and metals PCMs. However, if  $\lambda$  is not high enough, the release of the stored heat could be affected [95]. For this reason, the formulations of CPCMs seeks also for an enhancement on this property in the final material. Many support-substances and structures were employed, the common factor is the high thermal conductivity of at least one component: expanded graphite [75, 76], nickel foam [63] or porous aluminum nitride [64]. Additives are also employed to the  $\lambda$  enhancement:  $\text{Fe}_3\text{O}_4$  nanoparticles [65], copper foam fins [89], graphene nanoplates [49], among many others. A novel paraffin composite resulted with a high thermal conductivity around  $1.46 \text{ W/(m}\cdot\text{K)}$  by adding expanding graphite to the formulation [75] while a polyethylene glycol based CPCM reached  $2.04 \text{ W/}$

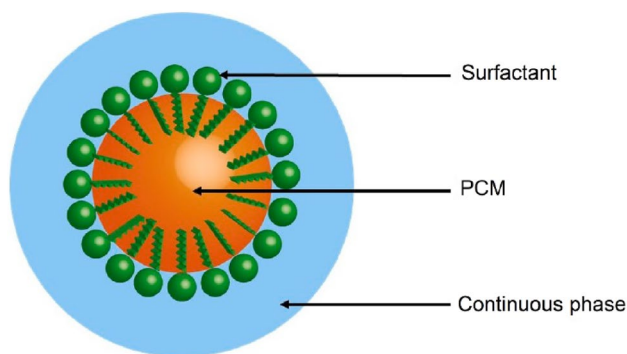


**Fig. 21** The structure of the PCM emulsion [105]

(m·K) with graphene nanoplates [49]. However, is not the form (porous structure or nanoparticle additives) of the component which delivers an increase on the final CPCM, but its own thermal conductivity and the employed amount, or even the nanoparticle size [96, 97]. Summary.

Recently, novel CPCMs are being formulated for different storage-integrated cooling technologies such as buildings [98, 99], batteries thermal management [80, 100], heat dissipation within electronic devices [50], among others. Galazutdinova and coauthors [41] developed a new inorganic CPCM based on  $\text{MgCl}_2 \cdot 6\text{H}_2\text{O}$  impregnated into expanded graphite matrix to increase their thermal conductivity, for passive thermal control of lithium-ion battery packs (Fig. 20).

In addition, the reuse of wastes and by-products as phase change materials (PCMs) promotes the implementation of circular economy [93]. Since was demonstrated that inorganic and organic CPCMs are efficient for the regulation of temperature gradient and for preserving stability of the batteries [41], a new field of application and reuse of industrial waste set up. In this sense, a CPCM composed by a mixture of bischofite and  $\text{Mg}(\text{NO}_3)_2 \cdot 6\text{H}_2\text{O}$  as PCM, and expanded graphite as support material was also employed for management of LIBs with excellent results [41].

## Slurries

Slurries are considered as one of the promising cooling technologies to increase the efficiency of the refrigeration sector [101, 102]. Slurries are a binary system that consists of carrier fluid and solid particles, and it can function as both a heat transfer fluid (HTF) and an energy storage medium [103]. Compared to traditional latent heat storage, the slurry system can possess higher heat conductivity and storage capacity, and better transportable fluidity without leakage [104].

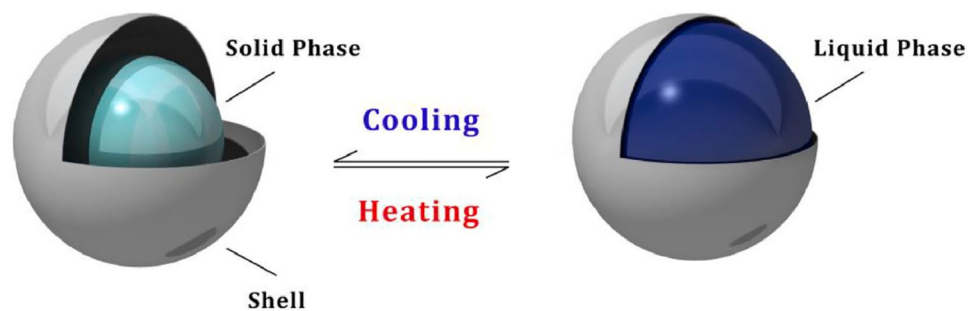
## Classification and properties

Based on the combination of the continuous phase and dispersed phase, the slurries that are utilized in the cooling application can be classified into the following five types.

### PCM emulsion (PCME) slurry

A PCM emulsion slurry, also known as phase change dispersion (PCD), can be defined as a mixture of PCM and carrier fluid. As depicted in Fig. 21, the PCM particle is not soluble but directly dispersed in the continuous fluid phase with the aid of suitable surfactants, such as sodium dodecyl sulfate (SDS), Tween, and Span [105–107]. PCME has the advantages of simple formulation, negligible thermal resistance at the interface, and low cost. Therefore, it has been widely studied for cooling and heating systems and solar energy harvesting [108, 109]. Paraffins, such as n-tetradecane and n-hexadecane, are generally adopted as PCM drops in this type of slurry, and water and oil are normally utilized as the carrier fluid. Liu et al. [110] fabricated two different paraffin based PCMEs with melting temperature of 29 °C and 38 °C. The cooling performance for the photovoltaic/thermal (P/T) systems were evaluated and a superior energy efficiency improvement of the P/T system was obtained against adopting water-cooled method. In [111], an n-hexadecane based PCME was designed for a pilot thermal energy storage system. The emulsion characterized a good dynamic stability and presented a much higher thermal storage capacity and a high efficiency of cold release compared to the water. Considering the non-sustainability and flammability of the paraffines, efforts have been made to investigate organic PCM drops such as fatty acids and alcohols. Salla et al. [112] succeeded in preparing an emulsion based on stearic acid via phase inversion composition (PIC) method. Owing to the increased free energy of the particles, the achieved melting temperature of the material was 3 to 4 °C lower than those of pure oil phases. In [113], lauric acid in silicon oil emulsion was investigated using the PIC method considering the production efficiency and cost effectiveness. Their test results indicated that the emulsion exhibited high storage stability and low supercooling, making it a promising candidate for application in thermal energy storage. On the other hand, Xu et al. [114] adopted alcohol as droplets to form an emulsion with polyalphaolefin. Both thermal conductivity and dynamic viscosity of the emulsion were tested and found to increase with alcohol loadings. In another study [115], Cetyl alcohol-in-water emulsion was produced following a solvent-assisted method. It was reported that when 8 wt.% content of dispersed phase was contained in the emulsion, a 20% enhancement in the energy storage capacity was obtained compared to that of water.

**Fig. 22** Schematic of encapsulated PCM [102]



Despite the attractive characteristics exhibited for working as efficient cooling media, the main challenges with the PCME slurry are instability and supercooling [108, 116]. To overcome these shortcomings, various functional materials have been investigated and added into the emulsion formation. In [117], the influence of graphene oxide and reduced graphene oxide on the stability of paraffine emulsions was tested. Through multiple storage and freeze–thaw cycles, no phase separation or coalescence was observed, and the stability of emulsions was verified. The combination of different surfactants was also adopted to develop stable PCM emulsions. As depicted in [118], an optimal formulation of Polyethylene glycol dodecyl ether and Tween 60 at 6:4 mass ratio could maintain a high stability of 25% (w/w) n-hexadecane emulsions when mixed with the PCM at an 11:20 mass ratio. To reduce the subcooling degree, single wall carbon nanohorns (SWCNHs) were investigated and mixed with paraffin/water emulsion [119]. About 2 °C or below of the subcooling was achieved by the addition of 0.01 wt% of the SWCNHs. As another effective nucleating agent, hydrophobic nano SiO<sub>2</sub> was also studied and tested [120, 121]. One study demonstrated that the subcooling degree of n-hexadecane in water emulsions could be controlled approximately 1 °C when the agent centration was from 1 wt% to 2 wt%.

### One-component PCM slurry

Ice slurry is the representative material in this category which refers to a homogenous mixture of ice microcrystals and carrier liquid (water) [122]. It has a high energy storage density compared to cold water and excellent fluidity compared to conventional ice like crushed ice and ice flakes [122, 123]. Moreover, ice slurry can provide long chilling times and sufficient heat transfer performance and avoid causing physical damage to the cooling product. Therefore, it has been widely investigated and applied in refrigeration and cold storage system [122, 124]. The slurries, slush nitrogen and slush hydrogen, can also be classified into this category, however, different preparation methods against that of slurry ice are needed for these materials [125].

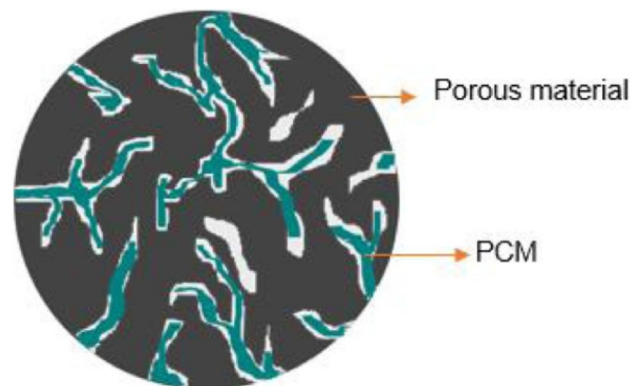


**Fig. 23** Typical representation of a shape-stabilised PCM [139]

The main shortcoming of one-component PCM slurry is subcooling, and foreign particles have been added to act as nuclei to solve the problem. Zou et al. [126] tested the ice slurry making characteristics with the introduction of the iron oxide nanoparticles and MgCl<sub>2</sub>, and the results showed that the subcooling degree was reduced by 55.80% and 37.52%, respectively. Nanoparticles, such as Al<sub>2</sub>O<sub>3</sub> and SiO<sub>2</sub> were also investigated and added into pure water to improve the nucleation of the ice slurries [127]. Additionally, to solve the supercooling in food-grade contexts, edible nucleus-chitosan was used in an ice slurry formation, and its feasibility in eliminating the subcooling degree was confirmed in [128].

### Encapsulated PCM slurry

Encapsulated PCM slurries are the suspension of PCM particles in carrier fluid where PCM particles are encapsulated into a shell [129]. Referring to Fig. 22, the particles can be solid, liquid, gas, or even multiphasic, and the encapsulation of particles can be conducted from micro (1 > μm) MPCM to nanoscale (1–1000 nm) NPCM level. The shell of PCM capsules which is generally a polymer, protects the core material from interacting with a carrier fluid, thereby enhancing the stability of the materials and avoiding particle aggregation. Furthermore, this technology can prevent

leakage during phase changes and increase the conductivity and surface-area-to-volume ratio [130]. The possibility of using different types of PCMs in one slurry system is another advantage of this technology to facilitate their application with more flexibility. Encapsulation of dimethyl adipate into a polymer shell using in-situ polymerisation was conducted in [129]. The produced NPCM possessed a melting temperature of 6.40 °C, with a latent heat potential of 80.2 J/g. Boldoo et al. [131] focused on the stearic acid (SAC) and stearyl alcohol (SAL) as the phase change materials and presented their potential to form efficient MPCM slurries for thermal energy storage. Among them, the SAL based slurry demonstrated superior performance owing to its higher melting and solidification latent heat energies. Alternatively, Dixit [132] et al. [131] experimentally tested the MPCM formed using hexadecane as PCMs and urea–formaldehyde as shell materials and proved their feasibility for energy storage applications.

The main issues of using encapsulated PCM slurry in working fluids is stratification and creaming [102]. The size and density of the capsules need to be investigated against the properties of the carrier fluid to make the particles distribute homogeneously. To address these issues, Dixit et al. [132] introduced mixed surfactants sodium dodecyl sulfate/non-polar polyvinylpyrrolidone to the hexadecane based MPCM slurry synthesis. Negligible change in thermal properties of the slurry was observed after 100 thermal cycles (0

to 30 °C), indicating an appreciable stability with temperature fluctuations. To prevent the creaming phenomenon, a mixture of Polyvinyl alcohol (PVA) and SDS was adopted as a surfactant in [133]. A comparison study against a single surfactant revealed that a long-term emulsion stability could be achieved in the former case because of the appearance of a whitish layer at the top of the emulsion. On the other hand, the complex structure and high cost compared to that of other slurry technologies should be taken into account in the fabrication of encapsulated PCM slurry.

### Shape-stabilized PCM slurry

As shown in Fig. 23, shape-stabilised PCM slurries are formulated by infiltrating the PCM particles in a support material with a cross-linked porous structure. The same shape of the PCM in a solid state can be maintained by the supporting material in the phase change process and the leakage of the melted PCM from the porous structure can be prevented by the capillary and surface tension. Paraffine was normally adopted as core material in this type of PCMs, and the high-density polyethylene (HDPE), styrene–butadiene–styrene triblock copolymer, and silica are utilised as the support materials to trap the PCMs [134–136]. Alternatively, oleic acid was employed to form PCM slurries using macroporous polymers (polyHIPEs) as supporting matrices [137].

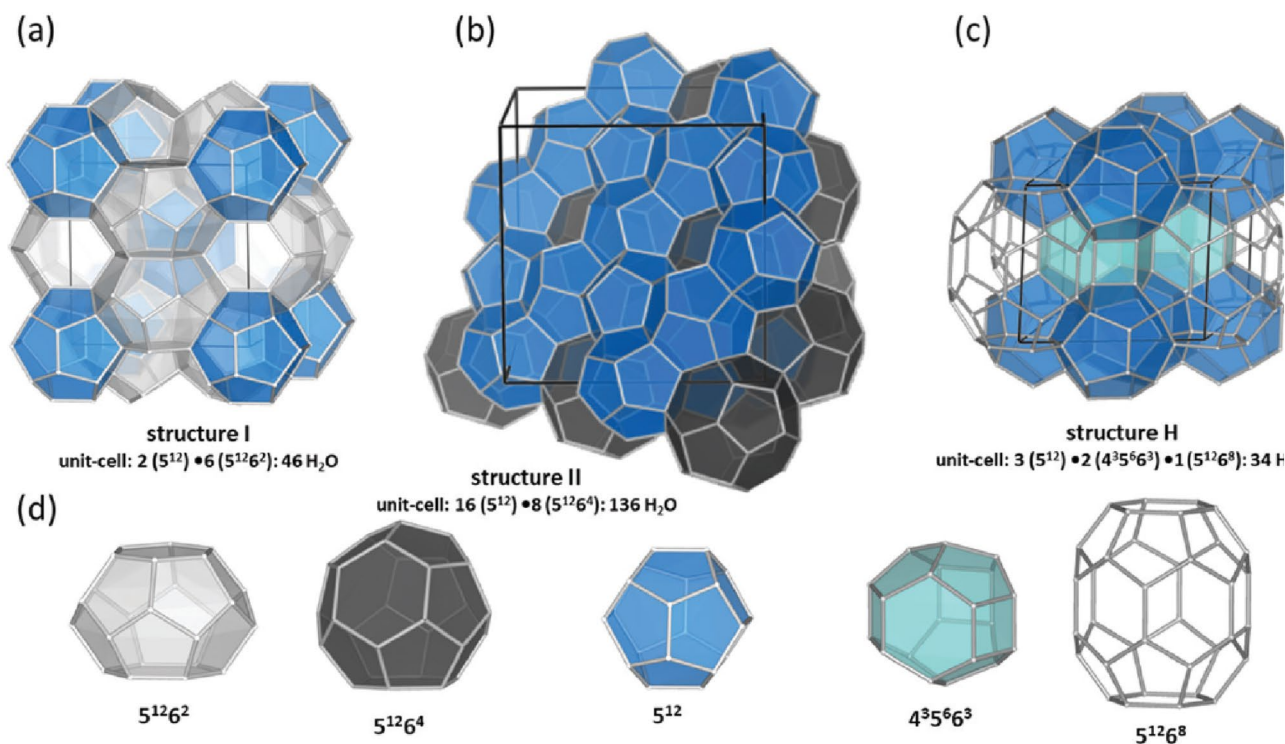


**Fig. 24** Three natural gas hydrate structures. **a** Structure I, **b** structure II, and **c** structure H, and **d** five different host water cages. The solid lines represent the unit-cell of each hydrate [140]

Referring to [138], dodecanol, known as lauryl acid, was also considered as PCMs and impregnated into the porous structure of diatomite to prepare shape-stabilised PCM.

Compared to the encapsulated PCM, the shape-stabilised PCM offers cost-effectiveness and simplicity in fabrication. However, difficulty in obtaining nanoscale particles and susceptibility to corrosion are the main shortcomings of this kind of slurry [139]. Additionally, based on the research listed above, another issue with using the PCM slurry is the lower dissociation enthalpy compared to pure PCM.

### Clathrate hydrate slurries

The clathrate hydrate slurries have ice-like crystalline structures in which small gas/liquid molecules are hosted by hydrogen-bonded water molecule cages. Under the Van der Waals attraction between the host and guest molecules, the stabilization of the hydrate can be achieved [104]. As shown in Fig. 24, the structures of clathrate hydrate are normally characterized into three types [140]. Among them, structure I (sI) hydrate is usually formed by smaller guest molecules (diameter: 0.4–0.55 nm), while structure II (sII) hydrate forms with larger guest molecules (diameter: 0.6–0.7 nm). On the other hand, small guest molecules used in forming sI and large molecules which diameter is in the range of 0.75–0.9 nm, are required simultaneously to generate the structure H (sH). Semi-clathrate hydrates of quaternary salts, in particular tetra-*n*-butyl ammonium bromide (TBAB), tetra-*n*-butyl ammonium chloride (TBAC), and tetra-*n*-butyl ammonium fluoride (TBAF) hydrates, are also commonly adopted for the application of cold storage and transportation [141, 142]. A considerable heat capacity in the formation and dissociation can be formed in this hydrate structure, and contrary to the traditional gas hydrate, the semi-clathrate hydrates can be shaped at ambient pressure and temperature.

The common guest gases for hydrate formation include hydrogen (H<sub>2</sub>), nitrogen (N<sub>2</sub>), carbon dioxide (CO<sub>2</sub>), methane (CH<sub>4</sub>), and ethane (C<sub>2</sub>H<sub>6</sub>) [143]. As more efforts have been taken in the development of environmentally friendly hydrate slurry, the guest materials with the properties of non-toxic, non-flammable, and low Global Warming Potential and Ozone Depletion Potential are becoming popular. Gas hydrate slurry formed by carbon dioxide (CO<sub>2</sub>) and water is one of the candidates [144, 145]. Owing to the high latent heat of fusion of over 500 kJ/kg and relatively high working temperature within the range 0–10 °C, the CO<sub>2</sub> hydrate-based refrigeration system has advantages in the improvement of the efficiency of cooling with a high value of Coefficient of Performance.

Despite attractive characteristics for operating as cold medium, subcooling, deviation from equilibrium condition, agglomeration, and slow formation kinetics are the main issues that hinder the application of clathrate

hydrate [146, 147]. Efforts have been made to solve these problems from both chemical and mechanical perspectives. In the chemical approach, thermodynamic promoters such as Cyclopentane (CP) and tetrahydrofuran (THF) were added into aqueous solution to shift the equilibrium profile of the hydrate formation towards milder conditions [148, 149]. From the kinetic point of view, SDS, amino acid, and Tween are typically adopted to enlarge the contacting area of the reactants and improve the hydrate formation rate [150–152]. Additionally, additives such as porous and high conduction particles were also employed in hydrate formation to enhance heat transfer [150, 153]. On the other hand, mechanical methods mainly include stirring, spraying, and bubbling [154–156]. The interface of reactants can be continually renewed under these external stimulations, achieving enhancement of mass and heat transfer.

### Selection criteria

Referring to the above literature review, various types of slurries have been investigated for cooling and storage purposes; however, the selection of the technologies should be conducted strictly connected to the application contexts considering the following criteria:

- **Temperature:** the formation and dissociation temperature of the slurries need to be selected according to the temperature requirements in the application scenarios being analyzed.
- **Fusion heat:** for the storage application, the heat absorbed or released by the phase change or reaction needs to be considered to decide the mass of the materials and capacity of the related system.
- **Availability:** although various technologies have been proposed and investigated, however, ice slurries and hydrate slurries are still the most used commercialized materials. The development stage of the materials needs to be kept in mind for reducing the risk in applications.
- **Affordability:** the materials need to be cost-effective in the preparation, especially for utilization in large-scale systems and industrial applications.
- **Environmental influence:** to tackle climate change and achieve net-zero in the energy sector, the global warming potential and ozone depletion potential need to be considered in the selection of composite materials for the formulation of the slurries.

## Economic analysis and evaluation sustainability

Although in the development of novel thermal energy storage (TES) technologies economic and sustainable aspects are crucial, they still represent a research gap in literature [157].

Regarding the economic aspects, to the best of authors knowledge only a few studies were already published in the literature especially regarding PCM composites and hydrates. Jeon et al. [158] studies the effect of shape-stabilized PCMs in cementitious composites for building applications to reduce both heating and cooling demand. PureTemp® and coconut oil were selected as storage materials thermal energy storage aggregates and an economic analysis was conducted to estimate the energy savings. The results showed that coconut oil, although it has a lower latent heat was more economically effective. Another study concerning the economic analysis was published by Yang et al. [159]. A techno-economic analysis was applied on the charging and discharging on a meta foam composite PCM for cold TES applications and the result showed that using those PCM has several benefits in terms of energy saving with a payback period of less than two years. Moreover, considering Beijing as a case study, results showed that it is possible achieving up to \$425.6 k of savings using a metal-foam-cored plate heat exchanger (12 m<sup>3</sup>) compared to water as storage medium.

In terms of environmental aspects, further is needed to overcome actual barriers of TES and support their market deployment. Moreover, the concept of circularity is gaining a high interest in the development of new materials and processes. In the field of TES, most of the materials are based on fossil fuels or natural resources and in recent years bio-PCM has attracted a lot of research in literature [160]. These PCM has an organic base and made of sustainable and eco-friendly bio-sources or by-products including oils or animal fats. Alcohols, fatty acids, glycols, and esters are the main types of bioPCMs [161]. The main drawbacks bio-PCM includes low-thermal conductivity, flammability, and degradation. Nevertheless, they represent a sustainable option to positively affect the environmental impact of TES technologies.

## Conclusions

The present work aims at the depth description of the main composite materials used in renewable/thermally driven and storage-integrated cooling technologies. Three family of composite materials, composite sorbents, composite PCMs and slurries were analyzed from the point of view of the main physical – chemical properties and based on their classification. An evaluation of economic analysis and sustainability was also presented. The paper showed that the research activities is still in course to improve the characteristic of these family of materials nevertheless the room is empty in terms of study of economic and sustainable aspects.

**Acknowledgements** The authors at University of Lleida would like to thank the Catalan Government for the quality accreditation given to their research group GREiA (2021 SGR 01615). GREiA is a certified agent TECNIO in the category of technology developers from the Government of Catalonia. This work is partially supported by ICREA under the ICREA Academia programme. This project has received funding from ThumbsUp (Thermal energy storage solUTions to optimally Manage BuildingS and Unlock their grid balancing and flexibility Potential). ThumbsUP is a Horizon Europe Project supported by the European Commission under contract No. 101096921.

**Author contributions** For research articles with several authors, a short paragraph specifying their individual contributions must be provided. The following statements should be used “Conceptualization, V. Brancato, L. F. Cabeza, S. Ushak, Y. Li; methodology, Y. Zhang, E. Borri; writing—original draft preparation, Y. Zhang, E. Borri, Y. Milian; D. Li; writing—review and editing, V. Brancato, L. F. Cabeza, S. Ushak, Y. Li, A. Frazzica, M. Grageda; visualization, Y. Li.; supervision, V. Brancato; project administration, V. Brancato.; funding acquisition, V. Brancato, L. F. Cabeza, S. Ushak, Y. Li. All authors have read and agreed to the published version of the manuscript.

**Funding** This project has received funding from the European Union’s Horizon 2020 research and innovation programme under grant agreement CO-COOL (101007976). Authors acknowledge to ANID/PUENTE No 1522A0006 and ANID/FONDECYT REGULAR No 1231721 projects. This work was partially funded by the Ministerio de Ciencia e Innovación de España [(PID2021-123511OB-C31—MCIU/AEI/FEDER, UE) (RED2022-134219-T)]. The authors at the University of Birmingham gratefully acknowledge the financial supports from the Engineering and Physical Sciences Research Council (EPSRC) of the UK (EP/T022701/1).

**Data availability** Data is available under request.

## Declarations

**Conflicts of interest** The authors declare no conflict of interest.

**Open Access** This article is licensed under a Creative Commons Attribution 4.0 International License, which permits use, sharing, adaptation, distribution and reproduction in any medium or format, as long as you give appropriate credit to the original author(s) and the source, provide a link to the Creative Commons licence, and indicate if changes were made. The images or other third party material in this article are included in the article’s Creative Commons licence, unless indicated otherwise in a credit line to the material. If material is not

included in the article's Creative Commons licence and your intended use is not permitted by statutory regulation or exceeds the permitted use, you will need to obtain permission directly from the copyright holder. To view a copy of this licence, visit <http://creativecommons.org/licenses/by/4.0/>.

## References

- Rehfeldt, M., Fleiter, T., Toro, F.: A bottom-up estimation of the heating and cooling demand in European industry. *Energy Effic.* **11**, 1057–1082 (2018). <https://doi.org/10.1007/s12053-017-9571-y>
- Zhang, Y., Palamara, D., Palomba, V., Calabrese, L., Frazzica, A.: Performance analysis of a lab-scale adsorption desalination system using silica gel/LiCl composite. *Desalination* (2023). <https://doi.org/10.1016/j.desal.2022.116278>
- Cárdenas-Ramírez, C., Gómez, M.A., Jaramillo, F., Fernández, A.G., Cabeza, L.F.: Thermal reliability of organic-organic phase change materials and their shape-stabilized composites. *J. Energy Storage* (2021). <https://doi.org/10.1016/j.est.2021.102661>
- Dubey, K.K., Mishra, R.S.: Solar integrated combined cooling-power generation systems for waste heat recovery using different energy efficient materials. *Int. J. Digit. Signal Smart Syst.* **5**, 125–136 (2021). <https://doi.org/10.1504/IJDSST.2021.114556>
- Scapino, L., Zondag, H.A., Van Bael, J., Diriken, J., Rindt, C.C.M.: Sorption heat storage for long-term low-temperature applications: a review on the advancements at material and prototype scale. *Appl. Energy* **190**, 920–948 (2017). <https://doi.org/10.1016/j.apenergy.2016.12.148>
- Li, W., Klemeš, J.J., Wang, Q., Zeng, M.: Salt hydrate – based gas-solid thermochemical energy storage : Current progress, challenges, and perspectives. *Renew. Sustain. Energy Rev.* (2022). <https://doi.org/10.1016/j.rser.2021.111846>
- Yu, N., Wang, R.Z., Wang, L.W.: Sorption thermal storage for solar energy. *Prog. Energy Combust. Sci.* **39**, 489 (2013)
- Thommes, M., Kaneko, K., Neimark, A.V., Olivier, J.P., Rodriguez-Reinoso, F., Rouquerol, J., Sing, K.S.W.: Physisorption of gases, with special reference to the evaluation of surface area and pore size distribution (IUPAC Technical Report). *Pure Appl. Chem.* **87**, 1051–1069 (2015). <https://doi.org/10.1515/pac-2014-1117>
- Yu, N., Wang, R.Z., Lu, Z.S., Wang, L.W., Ishugah, T.F.: Evaluation of a three-phase sorption cycle for thermal energy storage. *Energy* **67**, 468–478 (2014). <https://doi.org/10.1016/j.energy.2013.12.044>
- Aristov, Y.I., Restuccia, G., Cacciola, G., Parmon, V.N.: A family of new working materials for solid sorption air conditioning systems. *Appl. Therm. Eng.* **22**, 191–204 (2002). [https://doi.org/10.1016/S1359-4311\(01\)00072-2](https://doi.org/10.1016/S1359-4311(01)00072-2)
- Zhang, Y.N., Wang, R.Z., Zhao, Y.J., Li, T.X., Riffat, S.B., Wajid, N.M.: Development and thermochemical characterizations of vermiculite/SrBr<sub>2</sub> composite sorbents for low-temperature heat storage. *Energy* **115**, 120–128 (2016). <https://doi.org/10.1016/j.ENERGY.2016.08.108>
- Zhang, Y., Wang, R., Li, T., Zhao, Y.: Thermochemical characterizations of novel vermiculite-LiCl composite sorbents for low-temperature heat storage. *Energies* (2016). <https://doi.org/10.3390/en9100854>
- Zhang, Y., Wang, R.: Sorption thermal energy storage: concept, process, applications and perspectives. *Energy Storage Mater.* **27**, 352–369 (2020). <https://doi.org/10.1016/j.ensm.2020.02.024>
- Yin, Y., Qu, Z.G., Zhang, J.F.: International Journal of Heat and Mass Transfer Multiple diffusion mechanisms of shale gas in nanoporous organic matter predicted by the local diffusivity lattice Boltzmann model. *Int. J. Heat Mass Transf.* (2019). <https://doi.org/10.1016/j.ijheatmasstransfer.2019.118571>
- Mi, L., Jiang, H., Li, J.: The impact of diffusion type on multi-scale discrete fracture model numerical simulation for shale gas. *J. Nat. Gas. Sci. Eng.* **20**, 74–81 (2014). <https://doi.org/10.1016/j.jngse.2014.06.013>
- Thu, K., Saha, B.B., Chakraborty, A., Chun, W.G., Ng, K.C.: Study on an advanced adsorption desalination cycle with evaporator-condenser heat recovery circuit. *Int. J. Heat Mass Transf.* **54**, 43–51 (2011). <https://doi.org/10.1016/j.ijheatmasstransfer.2010.09.065>
- Thu, K., Chakraborty, A., Kim, Y.-D., Myat, A., Saha, B.B., Ng, K.C.: Numerical simulation and performance investigation of an advanced adsorption desalination cycle. *Desalination* **308**, 209–218 (2013). <https://doi.org/10.1016/j.desal.2012.04.021>
- Woo, S.-Y., Lee, H.-S., Ji, H., Moon, D.-S., Kim, Y.-D.: Silica gel-based adsorption cooling cum desalination system: Focus on brine salinity, operating pressure, and its effect on performance. *Desalination* **467**, 136–146 (2019). <https://doi.org/10.1016/j.desal.2019.06.016>
- Wei Benjamin Teo, H., Chakraborty, A., Fan, W.: Improved adsorption characteristics data for AQSOA types zeolites and water systems under static and dynamic conditions. *Microporous Mesoporous Mater.* **242**, 109–117 (2017). <https://doi.org/10.1016/j.micromeso.2017.01.015>
- Teo, H.W.B., Chakraborty, A., Han, B.: Water adsorption on CHA and AFI types zeolites: Modelling and investigation of adsorption chiller under static and dynamic conditions. *Appl. Therm. Eng.* **127**, 35–45 (2017). <https://doi.org/10.1016/j.applthermaleng.2017.08.014>
- Han, B., Chakraborty, A.: Advanced cooling heat pump and desalination employing functional UiO-66 (Zr) metal-organic frameworks. *Energy Convers. Manag.* (2020). <https://doi.org/10.1016/j.enconman.2020.112825>
- Teo, H.W.B., Chakraborty, A., Kitagawa, Y., Kayal, S.: Experimental study of isotherms and kinetics for adsorption of water on Aluminium Fumarate. *Int. J. Heat Mass Transf.* **114**, 621–627 (2017). <https://doi.org/10.1016/j.ijheatmasstransfer.2017.06.086>
- Elsayed, E., AL-Dadah, R., Mahmoud, S., Anderson, P., Elsayed, A.: Experimental testing of aluminium fumarate MOF for adsorption desalination. *Desalination* (2020). <https://doi.org/10.1016/j.desal.2019.114170>
- Youssef, P.G., Dakkama, H., Mahmoud, S.M., AL-Dadah, R.K.: Experimental investigation of adsorption water desalination/cooling system using CPO-27Ni MOF. *Desalination* **404**, 192–199 (2017). <https://doi.org/10.1016/j.desal.2016.11.008>
- Karmakar, A., Prabakaran, V., Zhao, D., Chua, K.J.: A review of metal-organic frameworks (MOFs) as energy-efficient desiccants for adsorption driven heat-transformation applications. *Appl. Energy* (2020). <https://doi.org/10.1016/j.apenergy.2020.115070>
- Férey, G., Mellot-Draznieks, C., Serre, C., Millange, F., Dutour, J., Surblé, S., Margiolaki, I.: A chromium terephthalate-based solid with unusually large pore volumes and surface area. *Science* **1979**(309), 2040–2042 (2005). <https://doi.org/10.1126/science.1116275>
- Cabeza, L.F., Solé, A., Barreneche, C.: Review on sorption materials and technologies for heat pumps and thermal energy storage. *Renew. Energy* **110**, 3–39 (2017). <https://doi.org/10.1016/j.renene.2016.09.059>
- Wang, L.W., Wang, R.Z., Oliveira, R.G.: A review on adsorption working pairs for refrigeration. *Renew. Sustain. Energy Rev.* **13**, 518–534 (2009). <https://doi.org/10.1016/j.rser.2007.12.002>

29. Sun, B., Chakraborty, A.: Thermodynamic formalism of water uptakes on solid porous adsorbents for adsorption cooling applications. *Appl. Phys. Lett.* (2014). <https://doi.org/10.1063/1.4876922>
30. Bai, S., Ho, T.C., Ha, J., An, A.K., Tso, C.Y.: Study of the salinity effects on the cooling and desalination performance of an adsorption cooling cum desalination system with a novel composite adsorbent. *Appl. Therm. Eng.* (2020). <https://doi.org/10.1016/j.applthermaleng.2020.115879>
31. Elsayed, E., AL-Dadah, R., Mahmoud, S., Anderson, P.A., Elsayed, A., Youssef, P.G.: CPO-27(Ni), aluminium fumarate and MIL-101(Cr) MOF materials for adsorption water desalination. *Desalination* **406**, 25–36 (2017). <https://doi.org/10.1016/j.desal.2016.07.030>
32. Mohammed, R.H.: Pore-size engineered nanoporous silica for efficient adsorption cooling and desalination cycle. *NPJ Clean Water* (2021). <https://doi.org/10.1038/s41545-021-00129-y>
33. Adam, N.K.: The Adsorption of Gases and Vapours. *Nature* **155**, 154–155 (1945)
34. Yu, N., Wang, R.Z., Lu, Z.S., Wang, L.W.: Study on consolidated composite sorbents impregnated with LiCl for thermal energy storage. *Int. J. Heat Mass Transf.* **84**, 660–670 (2015). <https://doi.org/10.1016/j.ijheatmasstransfer.2015.01.065>
35. Hadiya, J.P., Shukla, A.K.N.: Thermal energy storage using phase change materials: A way forward. *Int. J. Global Energy Issues* **41**, 108–127 (2018). <https://doi.org/10.1504/IJGEL.2018.092311>
36. Milián, Y.E., Gutiérrez, A., Grágeda, M., Ushak, S.: A review on encapsulation techniques for inorganic phase change materials and the influence on their thermophysical properties. *Renew. Sustain. Energy Rev.* **73**, 983–999 (2017). <https://doi.org/10.1016/j.rser.2017.01.159>
37. Ushak, S., Gutierrez, A., Barreneche, C., Fernandez, A.I., Grágeda, M., Cabeza, L.F.: Reduction of the subcooling of bischofite with the use of nucleating agents. *Sol. Energy Mater. Sol. Cells* **157**, 1011–1018 (2016). <https://doi.org/10.1016/j.solmat.2016.08.015>
38. Gutierrez, A., Ushak, S., Galleguillos, H., Fernandez, A., Cabeza, L.F., Grágeda, M.: Use of polyethylene glycol for the improvement of the cycling stability of bischofite as thermal energy storage material. *Appl. Energy* **154**, 616–621 (2015). <https://doi.org/10.1016/j.apenergy.2015.05.040>
39. Khademi, A., Shank, K., Mehrjardi, S.A.A., Tiari, S., Sorrentino, G., Said, Z., Chamkha, A.J., Ushak, S.: A brief review on different hybrid methods of enhancement within latent heat storage systems. *J. Energy Storage* (2022). <https://doi.org/10.1016/j.est.2022.105362>
40. Methode Kalombe, R., Sobhansarbandi, S., Kevern, J.: Low-cost phase change materials based concrete for reducing deicing needs. *Constr. Build. Mater.* (2023). <https://doi.org/10.1016/j.conbuildmat.2022.129129>
41. Galazutdinova, Y., Al-Hallaj, S., Grágeda, M., Ushak, S.: Development of the inorganic composite phase change materials for passive thermal management of Li-ion batteries: material characterization. *Int. J. Energy Res.* **44**, 2011–2022 (2020). <https://doi.org/10.1002/er.5054>
42. Solangi, N.H., Mubarak, N.M., Karri, R.R., Mazari, S.A., Jatoi, A.S., Koduru, J.R., Dehghani, M.H.: MXene-based phase change materials for solar thermal energy storage. *Energy Convers. Manag.* (2022). <https://doi.org/10.1016/j.enconman.2022.116432>
43. Cabeza, L.F., Inés Fernández, A., Barreneche, C., Ushak, S.: PCM Storage. In: Yan, J. (ed.) *Handbook of Clean Energy Systems*. Wiley (2015)
44. Gutierrez, A., Ushak, S., Mamani, V., Vargas, P., Barreneche, C., Cabeza, L.F., Grágeda, M.: Characterization of wastes based on inorganic double salt hydrates as potential thermal energy storage materials. *Solar Energy Mater. Solar Cells* (2017). <https://doi.org/10.1016/j.solmat.2017.05.036>
45. Gutierrez, A., Miró, L., Gil, A., Rodríguez-aseguinolaza, J., Barreneche, C., Calvet, N., Py, X., Fernández, A.I., Grágeda, M., Ushak, S., Cabeza, L.F.: Advances in the valorization of waste and by-product materials as thermal energy storage (TES) materials. *Renew. Sustain. Energy Rev.* **59**, 763–783 (2016). <https://doi.org/10.1016/j.rser.2015.12.071>
46. Gao, D., Sun, Y., Mi, A., Gu, X.: Mineral-based form-stable phase change materials for thermal energy storage : a state-of-the art review. *Energy Storage Mater.* **46**, 100–128 (2022). <https://doi.org/10.1016/j.ensm.2022.01.003>
47. Singh, S., Gaikwad, K.K., Lee, Y.S.: Phase change materials for advanced cooling packaging. *Environ. Chem. Lett.* **16**, 845–859 (2018). <https://doi.org/10.1007/s10311-018-0726-7>
48. Awan, M.B., Ma, Z., Lin, W., Pandey, A.K., Tyagi, V.V.: A characteristic-oriented strategy for ranking and near-optimal selection of phase change materials for thermal energy storage in building applications. *J. Energy Storage.* (2023). <https://doi.org/10.1016/j.est.2022.106301>
49. Xu, C., Wang, W., Zhang, H., Fang, G.: Polyethylene glycol/polyvinyl butyral/graphene nanoplates as composite phase-change materials with high thermal conductivity. *Sol. Energy Mater. Sol. Cells* (2023). <https://doi.org/10.1016/j.solmat.2022.112093>
50. Cheng, Z., Chang, G., Xue, B., Xie, L., Zheng, Q.: Hierarchical Ni-plated melamine sponge and MXene film synergistically supported phase change materials towards integrated shape stability, thermal management and electromagnetic interference shielding. *J. Mater. Sci. Technol.* **132**, 132–143 (2023). <https://doi.org/10.1016/j.jmst.2022.05.049>
51. Rahimi, M., Azimi, N., Nouira, M., Shahsavari, A.: Experimental study on photovoltaic panels integrated with metal matrix sheets and bio-based phase change materials. *Energy* (2023). <https://doi.org/10.1016/j.energy.2022.125371>
52. Milian, Y.E., Ushak, S.: Influence of monomers and solvents in the direct sol-gel synthesis of LiNO<sub>3</sub> shape stabilized phase change materials. *Mater. Chem. Phys.* (2021). <https://doi.org/10.1016/j.matchemphys.2021.125089>
53. Ushak, S., Fernández, A.G., Grágeda, M.: Using molten salts and other liquid sensible storage media in thermal energy storage (TES) systems. In: Ushak, S. (ed.) *Advances in Thermal Energy Storage Systems: Methods and Applications*. Elsevier Inc (2015)
54. Fabiani, C., Santini, C., Barbanera, M., Giannoni, T., Rubino, G., Cotana, F., Pisello, A.L.: Phase change materials-impregnated biomass for energy efficiency in buildings: Innovative material production and multiscale thermophysical characterization. *J. Energy Storage* (2023). <https://doi.org/10.1016/j.est.2022.106223>
55. Wang, H., Deng, Y., Liu, Y., Wu, F., Wang, W., Jin, H., Zheng, J., Lei, J.: In situ preparation of light-driven cellulose-Mxene aerogels based composite phase change materials with simultaneously enhanced light-to-heat conversion, heat transfer and heat storage. *Compos. Part A Appl. Sci. Manuf.* (2022). <https://doi.org/10.1016/j.compositesa.2022.106853>
56. Liu, K., Zhao, H., Yuan, Z., Zhao, F., Chen, D., Shi, C.: Preparation and characterization of steel slag-based low, medium, and high-temperature composite phase change energy storage materials. *J. Energy Storage* (2023). <https://doi.org/10.1016/j.est.2022.106309>
57. Zhao, K., Wang, J., Xie, H., Guo, Z.: Microencapsulated phase change n-Octadecane with high heat storage for application in building energy conservation. *Appl. Energy* (2023). <https://doi.org/10.1016/j.apenergy.2022.120284>
58. Li, S., Wang, H., Gao, X., Niu, Z., Song, J.: Design of corn straw/paraffin wax shape-stabilized phase change materials with excellent thermal buffering performance. *J. Energy Storage.* (2023). <https://doi.org/10.1016/j.est.2022.106217>



59. Li, D., Tang, Y., Zuo, X., Zhao, X., Zhang, X., Yang, H.: Preparation of hierarchical porous microspheres composite phase change material for thermal energy storage concrete in buildings. *Appl. Clay Sci.* (2023). <https://doi.org/10.1016/j.clay.2022.106771>
60. Singh, A.K., Rathore, P.K.S., Sharma, R.K., Gupta, N.K., Kumar, R.: Experimental evaluation of composite concrete incorporated with thermal energy storage material for improved thermal behavior of buildings. *Energy* (2023). <https://doi.org/10.1016/j.energy.2022.125701>
61. Fan, R., Zheng, N., Sun, Z.: A modified method to quantify the photo-thermal conversion efficiency of shape-stable phase change materials. *Sol. Energy Mater. Sol. Cells* (2022). <https://doi.org/10.1016/j.solmat.2021.111572>
62. Shi, X., Meng, Y., Bi, R., Wan, Z., Zhu, Y., Rojas, O.J.: Enabling unidirectional thermal conduction of wood-supported phase change material for photo-to-thermal energy conversion and heat regulation. *Compos. B Eng.* (2022). <https://doi.org/10.1016/j.compositesb.2022.110231>
63. Yang, R., Huang, X., Zhao, G., Liu, Z., Wang, G.: Ni@rGO into nickel foam for composite polyethylene glycol and erythritol phase change materials. *Chem. Eng. J.* (2023). <https://doi.org/10.1016/j.cej.2022.138900>
64. Wang, L., Kong, X., Ren, J., Fan, M., Li, H.: Novel hybrid composite phase change materials with high thermal performance based on aluminium nitride and nanocapsules. *Energy* (2022). <https://doi.org/10.1016/j.energy.2021.121775>
65. Zhang, J., Xu, Y., Li, X., Li, H., Yao, C., Chen, S., Xu, F.: Leak-free, high latent heat and self-cleaning phase change materials supported by layered cellulose/Fe<sub>3</sub>O<sub>4</sub> skeleton for light-to-thermal energy conversion. *Energy Convers. Manag.* (2022). <https://doi.org/10.1016/j.enconman.2022.115357>
66. Yu, K., Jia, M., Yang, Y., Liu, Y.: A clean strategy of concrete curing in cold climate: solar thermal energy storage based on phase change material. *Appl. Energy* (2023). <https://doi.org/10.1016/j.apenergy.2022.120375>
67. Wang, J., Yin, Y., Wang, Y., Huang, J.: Thermal performance analysis of multi-stage cold storage packed bed with modified phase change material based on Na<sub>2</sub>SO<sub>4</sub>·10H<sub>2</sub>O. *Appl. Therm. Eng.* (2023). <https://doi.org/10.1016/j.applthermaleng.2022.119666>
68. Ye, R., Jiang, H., Wang, J., Yang, X., Shu, X.: Fabrication and characteristics of eutectic hydrated salts/fumed silica composite as form-stable phase change materials for thermal energy storage. *Sol. Energy Mater. Sol. Cells* (2022). <https://doi.org/10.1016/j.solmat.2022.111584>
69. Lee, W., Seo, M., Kim, J.: Ultra-high thermal conductivity and mechanical properties of a paraffin composite as a thermal conductive phase change materials for novel heat management. *Compos. Sci. Technol.* (2022). <https://doi.org/10.1016/j.compscitech.2022.109282>
70. Lv, L., Wang, Y., Ai, H., Chen, T., Zhang, X., Song, S.: 3D graphene/silver nanowire aerogel encapsulated phase change material with significantly enhanced thermal conductivity and excellent solar-thermal energy conversion capacity. *J. Mater. Chem. A Mater.* **10**, 7773–7784 (2022). <https://doi.org/10.1039/D1TA10037H>
71. Li, W.Q., Zhang, T.Y., Li, B.B., Xue, Z.R., Wang, H., Zhang, D.: Enhanced energy management performances of passive cooling, heat storage and thermoelectric generator by using phase change material saturated in metal foam. *Int. J. Ther. Sci.* (2023). <https://doi.org/10.1016/j.ijthermalsci.2022.107869>
72. Gad, R., Mahmoud, H., Ookawara, S., Hassan, H.: Evaluation of thermal management of photovoltaic solar cell via hybrid cooling system of phase change material inclusion hybrid nanoparticles coupled with flat heat pipe Salvage value. *J. Energy Storage* (2023). <https://doi.org/10.1016/j.est.2022.106185>
73. Ge, X., Li, X., Jin, Y., Zhang, G., Deng, J., Ge, J.: Experimental investigation on thermal management system of composite phase change material coupled with serpentine tubes for battery module. *Appl. Therm. Eng.* (2023). <https://doi.org/10.1016/j.applthermaleng.2022.119501>
74. Liu, J., Fan, Y., Xie, Q.: An experimental study on the thermal performance of mixed phase change materials-based battery cooling system. *J. Energy Storage* (2022). <https://doi.org/10.1016/j.est.2021.103839>
75. Zhang, C., Zheng, X., Xie, N., Fang, Y., Zhang, Z., Gao, X.: Form-stable flexible composite multi-phase change material with high latent heat and enhanced thermal conductivity for thermal management. *J. Energy Storage* (2023). <https://doi.org/10.1016/j.est.2022.106364>
76. Ma, C., Zhang, Y., Hu, S., Liu, X., He, S.: A copper nanoparticle enhanced phase change material with high thermal conductivity and latent heat for battery thermal management. *J. Loss Prev. Process Ind.* (2022). <https://doi.org/10.1016/j.jlp.2022.104814>
77. Marin, P., Saffari, M., de Gracia, A., Zhu, X., Farid, M.M., Cabeza, L.F., Ushak, S.: Energy savings due to the use of PCM for relocatable lightweight buildings passive heating and cooling in different weather conditions. *Energy Build.* (2016). <https://doi.org/10.1016/j.enbuild.2016.08.007>
78. Villalobos, I., De Gracia, A., Chafer, M., Cabeza, L.F., Ushak, S.: Experimental Comparison of Passive Heating/Cooling Space in Lightweight Buildings with Potential Application in Mining Camps. *IOP Conf. Series Earth Environ. Sci.* (2020). <https://doi.org/10.1088/1755-1315/503/1/012083>
79. Vega, M., Llantoy, N., Chafer, M., Ushak, S., Cabeza, L.F.: Life cycle assessment of the inclusion of phase change materials in lightweight buildings. *J. Energy Storage* (2022). <https://doi.org/10.1016/j.est.2022.105903>
80. Galazutdinova, Y., Vega, M., Grágeda, M., Cabeza, L.F., Ushak, S.: Preparation and characterization of an inorganic magnesium chloride / nitrate / graphite composite for low temperature energy storage. *Sol. Energy Mater. Sol. Cells* **175**, 60–70 (2018). <https://doi.org/10.1016/j.solmat.2017.09.046>
81. Khobragade, S., Devanuri, J.K.: Phase change material thermal response under simultaneous charging and discharging process in an annular finned storage system with orientations: An experimental study. *Int. J. Thermof.* (2023). <https://doi.org/10.1016/j.ijft.2022.100256>
82. Zhang, H., Ling, Z., Zhou, S., Fang, X., Zhang, W.: Preparation and characteristic of wood-based inorganic composite phase change material with effective anisotropic thermal conductivity for thermal energy storage. *Solar Energy Mater. Solar Cells* (2023). <https://doi.org/10.1016/j.solmat.2022.112172>
83. Rathgeber, C., Schmit, H., Miró, L., Cabeza, L.F., Gutierrez, A., Ushak, S.N., Hiebler, S.: Enthalpy-temperature plots to compare calorimetric measurements of phase change materials at different sample scales. *J. Energy Storage* (2018). <https://doi.org/10.1016/j.est.2017.11.002>
84. Milián, Y.E., Ushak, S.: Development of shape stabilized thermal energy storage materials based on inorganic chloride salts by direct sol-gel method. *ACTA NOVA*. **9**, 754–772 (2010)
85. Rathgeber, C., Schmit, H., Miró, L., Cabeza, L.F., Gutierrez, A., Ushak, S.N., Hiebler, S., Hauer, A.: Analysis of supercooling of phase change materials with increased sample size – Comparison of measurements via DSC, T-History and at pilot plant scale. *GREENSTOCK 2015- The 13th International Conference on Energy Storage.* (2015)
86. Reddy, V.J., Yadav, J.S., Chattopadhyay, S.: Phase change material loaded form-stable composites for low temperature thermal buffering application. *Mater. Chem. Phys.* (2020). <https://doi.org/10.1016/j.matchemphys.2020.122859>

87. Li, Y., Zhou, S.H., Liang Di, M., Wang Tan, W., Zhi Zhu, Q.: Effect of Microstructure on Thermal Properties of EG/MA Shaped Composite Phase Change Materials. *Int. J. Thermophys.* (2023). <https://doi.org/10.1007/s10765-022-03130-w>
88. Gao, Y., He, F., Xu, T., Meng, X., Zhang, M., Yan, L., Gao, W.: Thermal performance analysis of sensible and latent heat thermal energy storage tanks: a contrastive experiment. *J. Build. Eng.* (2020). <https://doi.org/10.1016/j.jobe.2020.101713>
89. Zou, J., Meng, X.: Investigating the effect of distribution form of copper foam fins on the thermal performance improvement of latent thermal energy storage units. *Int. Commun. Heat Mass Trans.* (2023). <https://doi.org/10.1016/j.icheatmasstransfer.2022.106571>
90. Ushak, S., Fernández, A.G., Prieto, C., Grageda, M.: Advances in molten salt storage systems using other liquid sensible storage media for heat storage. In: Ushak, S. (ed.) *Advances in Thermal Energy Storage Systems: Methods and Applications*. Elsevier (2020)
91. Bastida, H., De la Cruz-Loredo, I., Ugalde-Loo, C.E.: Effective estimation of the state-of-charge of latent heat thermal energy storage for heating and cooling systems using non-linear state observers. *Appl. Energy* (2023). <https://doi.org/10.1016/j.apenergy.2022.120448>
92. Ushak, S., Vega, M., Lovera-Copa, J.A., Pablo, S., Lujan, M., Grageda, M.: Thermodynamic modeling and experimental verification of new eutectic salt mixtures as thermal energy storage materials. *Solar Energy Mater. Solar Cells* (2020). <https://doi.org/10.1016/j.solmat.2020.110475>
93. Ushak, S., Milian, Y.E., Marín, P.E., Grageda, M.: Applications of wastes based on inorganic salts as low-cost thermal energy storage materials. In: Ushak, S. (ed.) *Sustainable Material Solutions for Solar Energy Technologies: Processing Techniques and Applications*. Elsevier (2021)
94. Kong, Q.Q., Jia, H., Xie, L.J., Tao, Z.C., Yang, X., Liu, D., Sun, G.H., Guo, Q.G., Lu, C.X., Chen, C.M.: Ultra-high temperature graphitization of three-dimensional large-sized graphene aerogel for the encapsulation of phase change materials. *Compos. Part A Appl. Sci. Manuf.* (2021). <https://doi.org/10.1016/j.compositesa.2021.106391>
95. Ghosh, D., Ghose, J., Datta, P., Kumari, P., Paul, S.: Strategies for phase change material application in latent heat thermal energy storage enhancement: Status and prospect. *J. Energy Storage* (2022). <https://doi.org/10.1016/j.est.2022.105179>
96. Louis, S.P., Ushak, S., Milian, Y., Nemš, M., Nemš, A.: Application of Nanofluids in improving the performance of double-pipe heat exchangers—a critical review. *Materials* (2022). <https://doi.org/10.3390/ma15196879>
97. Wong-Pinto, L.S., Milian, Y., Ushak, S.: Progress on use of nanoparticles in salt hydrates as phase change materials. *Renew. Sustain. Energy Rev.* **122**, 109727 (2020)
98. Guo, R., Shan, L., Wu, Y., Cai, Y., Huang, R., Ma, H.: Phase-change materials for intelligent temperature regulation. *Mater. Today Energy* (2022). <https://doi.org/10.1016/j.mtener.2021.100888>
99. Saffari, M., De Gracia, A., Ushak, S., Cabeza, L.F.: Economic impact of integrating PCM as passive system in buildings using Fanger comfort model. *Energy Build* (2016). <https://doi.org/10.1016/j.enbuild.2015.12.006>
100. Galazutdinova, Y., Grágeda, M., Cabeza, L.F., Ushak, S.: Novel inorganic binary mixture for low-temperature heat storage applications. *Int. J. Energy Res.* **41**, 2356–2364 (2017). <https://doi.org/10.1002/er.3805>
101. Kauffeld, M., Wang, M.J., Goldstein, V., Kasza, K.E.: Ice slurry applications. *Int. J. Refrig.* **22**, 44 (2010). <https://doi.org/10.1016/j.ijrefrig.2010.07.018>
102. Ghasemi, K., Tasnim, S., Mahmud, S.: PCM, nano/microencapsulation and slurries: a review of fundamentals, categories, fabrication, numerical models and applications. *Sustain. Energy Technol. Assess.* (2022). <https://doi.org/10.1016/j.seta.2022.102084>
103. Borri, E., Hua, N., Sciacovelli, A., Wu, D., Ding, Y., Li, Y., Brancato, V., Zhang, Y., Frazzica, A., Li, W., Yu, Z., Milian, Y.E., Ushak, S., Grageda, M., Cabeza, L.F.: Phase change slurries for cooling and storage: an overview of research trends and gaps. *Energies* (2022). <https://doi.org/10.3390/en15196873>
104. Youssef, Z., Fournaison, L., Delahaye, A., Pons, M.: Management of vapor release in secondary refrigeration processes based on hydrates involving CO<sub>2</sub> as guest molecule Gestion de la libération de vapeur dans les processus frigorifiques secondaires à base d'hydrates contenant du CO<sub>2</sub> comme molécule invitée. *Int. J. Refrig.* **98**, 202–210 (2019). <https://doi.org/10.1016/j.ijrefrig.2018.11.017>
105. O'Neill, P., Fischer, L., Revellin, R., Bonjour, J.: Phase change dispersions: a literature review on their thermo-rheological performance for cooling applications. *Appl. Therm. Eng.* (2021). <https://doi.org/10.1016/j.applthermaleng.2021.116920>
106. Zhang, X., Niu, J., Zhang, S., Wu, J.-Y.: PCM in Water Emulsions: Supercooling Reduction Effects of Nano-Additives, Viscosity Effects of Surfactants and Stability. *Adv. Eng. Mater.* **17**, 181–188 (2015). <https://doi.org/10.1002/adem.201300575>
107. Zhang, Z., Yuan, Y., Zhang, N., Cao, X.: Thermophysical Properties of Some Fatty Acids/Surfactants as Phase Change Slurries for Thermal Energy Storage. *J. Chem. Eng. Data* **60**, 2495–2501 (2015). <https://doi.org/10.1021/acs.jced.5b00371>
108. Cabaleiro, D., Agresti, F., Fedele, L., Barison, S., Hermida-Merino, C., Losada-Barreiro, S., Bobbo, S., Piñeiro, M.M.: Review on phase change material emulsions for advanced thermal management: Design, characterization and thermal performance. *Renew. Sustain. Energy Rev.* **159**, 112238 (2022)
109. Li, Q., Qiao, G., Mura, E., Li, C., Fischer, L., Ding, Y.: Experimental and numerical studies of a fatty acid based phase change dispersion for enhancing cooling of high voltage electrical devices. *Energy* (2020). <https://doi.org/10.1016/j.ENERGY.2020.117280>
110. Liu, L., Niu, J., Wu, J.Y.: Improving energy efficiency of photovoltaic/thermal systems by cooling with PCM nano-emulsions: an indoor experimental study. *Renew. Energy* (2023). <https://doi.org/10.1016/j.renene.2022.12.090>
111. Liu, L., Zhang, X., Liang, H., Niu, J., Wu, J.Y.: Cooling storage performance of a novel phase change material nano-emulsion for room air-conditioning in a self-designed pilot thermal storage unit. *Appl. Energy* (2022). <https://doi.org/10.1016/j.apenergy.2021.118405>
112. Puupponen, S., Seppälä, A., Vartia, O., Saari, K., Ala-Nissilä, T.: Preparation of paraffin and fatty acid phase changing nanoemulsions for heat transfer. *Thermochim. Acta* (2015). <https://doi.org/10.1016/j.tca.2014.12.020>
113. Chen, Y., Mo, S., Chen, J., Yu, Y., Jia, L., Chen, Y.: A novel lauric acid in silicone oil phase change emulsion with enhanced thermal properties and stability prepared by emulsion inversion point method. *Sol. Energy Mater. Sol. Cells* (2024). <https://doi.org/10.1016/j.SOLMAT.2024.112855>
114. Xu, J., Yang, B., Hammouda, B.: Thermal conductivity and viscosity of self-assembled alcohol/polyalphaolefin nanoemulsion fluids. *Nanoscale Res. Lett.* (2011). <https://doi.org/10.1186/1556-276X-6-274>
115. Cabaleiro, D., Losada-Barreiro, S., Agresti, F., Hermida-Merino, C., Fedele, L., Lugo, L., Barison, S., Piñeiro, M.M.: Development and Thermophysical Profile of Cetyl Alcohol-in-water Nanoemulsions for thermal management. *Fluids* (2022). <https://doi.org/10.3390/fluids7010011>

116. Safari, A., Saidur, R., Sulaiman, F.A., Xu, Y., Dong, J.: A review on supercooling of Phase Change Materials in thermal energy storage systems. *Renew. Sustain. Rev.* **70**, 905 (2017)
117. Barison, S., Cabaleiro, D., Rossi, S., Kovtun, A., Melucci, M., Agresti, F.: Paraffin–graphene oxide hybrid nano emulsions for thermal management systems. *Colloids Surf A Physicochem Eng Asp* (2021). <https://doi.org/10.1016/j.colsurfa.2021.127132>
118. Liu, L., Niu, J., Wu, J.Y.: Formulation of highly stable PCM nano-emulsions with reduced supercooling for thermal energy storage using surfactant mixtures. *Sol. Energy Mater. Sol. Cells* (2021). <https://doi.org/10.1016/J.SOLMAT.2021.110983>
119. Agresti, F., Fedele, L., Rossi, S., Cabaleiro, D., Bobbo, S., Ischia, G., Barison, S.: Nano-encapsulated PCM emulsions prepared by a solvent-assisted method for solar applications. *Sol. Energy Mater. Sol. Cells* **194**, 268–275 (2019). <https://doi.org/10.1016/J.SOLMAT.2019.02.021>
120. Zhang, X., Niu, J., Wu Young, J.: Evaluation and manipulation of the key emulsification factors toward highly stable PCM-water Nano-emulsions for thermal energy storage. *Solar Energy Mater. Sol. Cells* (2021). <https://doi.org/10.1016/j.solmat.2020.110820>
121. Zhang, X., Niu, J., Wu, J.Y.: Development and characterization of novel and stable silicon nanoparticles-embedded PCM-in-water emulsions for thermal energy storage. *Appl. Energy* (2019). <https://doi.org/10.1016/j.apenergy.2019.01.159>
122. Zhang, C., Yang, L., Lin, W., Wei, J., Chen, J., Ma, Z.: Experimental investigation and life-cycle cost analysis of a cold storage enhanced vacuum cooling system using ice slurry. *Sustain. Energy Technol. Assess.* (2021). <https://doi.org/10.1016/j.seta.2021.101074>
123. Rezaei, M., Pakravan, H.A.: Thermo-fluidic characteristics of ice slurry flows in U-bend pipes for cold thermal energy storage. *J. Energy Storage* (2023). <https://doi.org/10.1016/j.est.2022.106224>
124. Zhou, Z., Zhang, G., Lu, W., Luo, M., Wu, Z.: Review on high ice packing factor (IPF) ice slurry: Fabrication, characterization, flow characteristics and applications. *J. Energy Storage* **81**, 110378 (2024)
125. Ma, F., Zhang, P.: A review of thermo-fluidic performance and application of shellless phase change slurry: Part 1—preparations, properties and applications. *Energy* **189**, 116246 (2019)
126. Zou, L., Zhang, X., Liu, W., Liu, L.: Experimental study on the preparation of binary ice by additives enhanced vacuum flash evaporation. *Int. J. Refriger.* (2021). <https://doi.org/10.1016/j.ijrefrig.2021.07.024>
127. Zhang, X.J., Wu, P., Qiu, L.M., Zhang, X.B., Tian, X.J.: Analysis of the nucleation of Nanofluids in the ice formation process. *Energy Convers. Manag.* **51**, 130–134 (2010). <https://doi.org/10.1016/J.ENCONMAN.2009.09.001>
128. Zhang, R., Cheng, Z., Ding, F., Hua, L., Fang, Y., Han, Z., Shi, J., Zou, X., Xiao, J.: Improvements in chitosan-based slurry ice production and its application in precooling and storage of *Pampus argenteus*. *Food Chem.* (2022). <https://doi.org/10.1016/j.foodchem.2022.133266>
129. Trivedi, G.V.N., Parameshwaran, R.: Micro/nanoencapsulation of dimethyl adipate with melamine formaldehyde shell as phase change material slurries for cool thermal energy storage. *Chem. Thermodynamics Ther. Anal.* (2022). <https://doi.org/10.1016/j.cta.2022.100037>
130. Alva, G., Lin, Y., Liu, L., Fang, G.: Synthesis, characterization and applications of microencapsulated phase change materials in thermal energy storage: a review. *Energy Build.* **144**, 276 (2017)
131. Boldoo, T., Chinnasamy, V., You, N., Cho, H.: Experimental analysis on thermal energy storage performance of micro-encapsulated stearic acid and stearyl alcohol PCM slurries; a comparative study. *J. Energy Storage* (2023). <https://doi.org/10.1016/j.est.2023.109218>
132. Dixit, P., Parvate, S., Reddy, V.J., Singh, J., Maiti, T.K., Dasari, A., Chattopadhyay, S.: Effect of surfactants on encapsulation of hexadecane phase change material in calcium carbonate shell for thermal energy storage. *J. Energy Storage* (2022). <https://doi.org/10.1016/j.est.2022.105491>
133. Al-Shannaq, R., Farid, M., Al-Muhtaseb, S., Kurdi, J.: Emulsion stability and cross-linking of PMMA microcapsules containing phase change materials. *Solar Energy Mater. Sol. Cells* (2015). <https://doi.org/10.1016/j.solmat.2014.08.036>
134. Zhang, P., Hu, Y., Song, L., Lu, H., Wang, J., Liu, Q.: Synergistic effect of iron and intumescent flame retardant on shape-stabilized phase change material. *Thermochim. Acta* (2009). <https://doi.org/10.1016/j.tca.2009.01.006>
135. Xiao, M., Feng, B., Gong, K.: Letters: Thermal performance of a high conductive shape-stabilized thermal storage material. *Solar Energy Mater. Sol. Cells* (2001). [https://doi.org/10.1016/S0927-0248\(01\)00056-3](https://doi.org/10.1016/S0927-0248(01)00056-3)
136. Miao, C., Lü, G., Yao, Y., Tang, G., Weng, D.: Preparation of shape-stabilized phase change materials as temperature-adjusting powder. *Front. Mater. Sci. China* (2007). <https://doi.org/10.1007/s11706-007-0051-8>
137. Mert, M.S., Mert, E.H., Pulko, I., Krajnc, P., Mert, H.H.: Form-stable oleic acid based polyHIPE/nanoclay framework supported composite phase change materials for low-temperature latent heat storage. *Ther. Sci. Eng. Progress.* (2024). <https://doi.org/10.1016/J.TSEP.2024.102569>
138. Fořt, J., Trník, A., Pavlíková, M., Pavlík, Z., Černý, R.: Fabrication of Dodecanol/Diatomite Shape-Stabilized PCM and Its Utilization in Interior Plaster. *Int. J. Thermophys.* (2018). <https://doi.org/10.1007/s10765-018-2459-z>
139. Cárdenas-Ramírez, C., Jaramillo, F., Gómez, M.: Systematic review of encapsulation and shape-stabilization of phase change materials, (2020)
140. Hassanpouryouzband, A., Joonaki, E., Vasheghani Farahani, M., Takeya, S., Ruppel, C., Yang, J., English, N.J., Schicks, J.M., Edlmann, K., Mehrabian, H., Aman, Z.M., Tohidi, B.: Gas hydrates in sustainable chemistry. *Chem. Soc. Rev.* **49**, 5225 (2020)
141. Kim, H., Zheng, J., Yin, Z., Babu, P., Kumar, S., Tee, J., Linga, P.: Semi-clathrate hydrate slurry as a cold energy storage and transport medium: rheological study, energy analysis and enhancement by amino acid. *Energy* (2023). <https://doi.org/10.1016/j.energy.2022.126226>
142. Liu, F.P., Li, A.R., Qing, S.L., Luo, Z.D., Ma, Y.L.: Formation kinetics, mechanism of CO<sub>2</sub> hydrate and its applications. *Renew. Sustain. Energy Rev.* **159**, 112221 (2022)
143. Sloan, E.D.: Fundamental principles and applications of natural gas hydrates. *Nature* **426**, 353 (2003)
144. Xie, N., Tan, C., Yang, S., Liu, Z.: Conceptual design and analysis of a novel CO<sub>2</sub> hydrate-based refrigeration system with cold energy storage. *ACS Sustain. Chem. Eng.* **7**, 1502–1511 (2019). <https://doi.org/10.1021/acssuschemeng.8b05255>
145. Hua, N., Lu, T., Yang, L., Mckeown, A., Yu, Z., Xu, B., Sciacovelli, A., Ding, Y., Li, Y.: Thermodynamic analysis and economic assessment of a carbon dioxide hydrate-based vapor compression refrigeration system using load shifting controls in summer. *Energy Convers. Manag.* (2022). <https://doi.org/10.1016/j.enconman.2021.114901>
146. Bhavya, T., Sai Kiran, B., Prasad, P.S.R.: The Role of Stirring and Amino Acid Mixtures to Surpass the Sluggishness of CO<sub>2</sub>Hydrates. *Energy Fuels* (2021). <https://doi.org/10.1021/acs.energyfuels.1c01830>
147. Li, D., Lu, T., Yu, Z., Ding, Y., Li, Y.: Effects of initial pressure and gas-water ratio on the CO<sub>2</sub> hydrate-based cold thermal energy storage under the gas-inducing agitation. *J. Energy Storage* (2024). <https://doi.org/10.1016/j.est.2024.110990>

148. Zheng, J.N., Yang, M.J., Liu, Y., Wang, D.Y., Song, Y.C.: Effects of cyclopentane on CO<sub>2</sub> hydrate formation and dissociation as a co-guest molecule for desalination. *J. Chem. Thermodynamics* (2017). <https://doi.org/10.1016/j.jct.2016.09.006>
149. Liu, J., Shi, S., Zhang, Z., Liu, H., Xu, J., Chen, G., Hou, J., Zhang, J.: Ab initio study of formation of the clathrate cage in the tetrahydrofuran hydrate. *J. Chem. Thermodynamics*. (2018). <https://doi.org/10.1016/j.jct.2018.01.007>
150. Mohammadi, A., Manteghian, M., Haghtalab, A., Mohammadi, A.H., Rahmati-Abkenar, M.: Kinetic study of carbon dioxide hydrate formation in presence of silver nanoparticles and SDS. *Chem. Eng. J.* (2014). <https://doi.org/10.1016/j.cej.2013.09.026>
151. Bavoh, C.B., Lal, B., Osei, H., Sabil, K.M., Mukhtar, H.: A review on the role of amino acids in gas hydrate inhibition, CO<sub>2</sub> capture and sequestration, and natural gas storage. *J. Nat. Gas. Sci. Eng.* **64**, 52 (2019)
152. Zhang, B.Y., Qiang, W.U., Sun, D.L.: Effect of surfactant Tween on induction time of gas hydrate formation. *J. China Univ. Min. Technol.* (2008). [https://doi.org/10.1016/S1006-1266\(08\)60004-8](https://doi.org/10.1016/S1006-1266(08)60004-8)
153. Kang, S.P., Lee, J.W.: Kinetic behaviors of CO<sub>2</sub> hydrates in porous media and effect of kinetic promoter on the formation kinetics. *Chem. Eng. Sci.* **65**, 1840–1845 (2010). <https://doi.org/10.1016/J.CES.2009.11.027>
154. Li, D., Lu, T., Yu, Z., Song, W., Ding, Y., Li, Y.: Experimental investigation on the promotion of CO<sub>2</sub> hydrate formation for cold thermal energy storage – Effect of gas-inducing stirring under different agitation speeds. *Green Energy Resourc.* (2023). <https://doi.org/10.1016/J.GERR.2024.100047>
155. Partoon, B., Sabil, K.M., Lau, K.K., Lal, B., Nasrifar, K.: Production of gas hydrate in a semi-batch spray reactor process as a means for separation of carbon dioxide from methane. *Chem. Eng. Res. Des.* (2018). <https://doi.org/10.1016/j.cherd.2018.08.024>
156. Bhati, A., Kar, A., Bahadur, V.: Analysis of CO<sub>2</sub> hydrate formation from flue gas mixtures in a bubble column reactor. *Sep. Purif. Technol.* (2024). <https://doi.org/10.1016/j.seppur.2023.125261>
157. Cabeza, L.F., de Gracia, A., Zsembinszki, G., Borri, E.: Perspectives on thermal energy storage research. *Energy* (2021). <https://doi.org/10.1016/j.energy.2021.120943>
158. Jeon, I.K., Azzam, A., Al Jebaei, H., Kim, Y.R., Aryal, A., Baltazar, J.C.: Effects of shape-stabilized phase change materials in cementitious composites on thermal-mechanical properties and economic benefits. *Appl. Therm. Eng.* (2023). <https://doi.org/10.1016/j.applthermaleng.2022.119444>
159. Yang, X., Bai, Q., Zhang, Q., Hu, W., Jin, L., Yan, J.: Thermal and economic analysis of charging and discharging characteristics of composite phase change materials for cold storage. *Appl. Energy* (2018). <https://doi.org/10.1016/j.apenergy.2018.05.063>
160. Junaid, M.F., Rehman, Z.U., Ijaz, N., Čekon, M., Čurpek, J., Babeker Elhag, A.: Biobased phase change materials from a perspective of recycling, resources conservation and green buildings. *Energy Build.* **270**, 112280 (2022)
161. Duquesne, M., Mailhé, C., Ruiz-Onofre, K., Achchaq, F.: Bio-sourced organic materials for latent heat storage: an economic and eco-friendly alternative. *Energy* (2019). <https://doi.org/10.1016/j.energy.2019.116067>

**Publisher's Note** Springer Nature remains neutral with regard to jurisdictional claims in published maps and institutional affiliations.